"DIFFUSION WEIGHTED MAGNETIC RESONANCE IMAGING FEATURES OF INTRACRANIAL LESIONS"

By

DR. PUNEET SHIRBUR M.B.B.S

Dissertation submitted to

BLDE UNIVERSITY, VIJAYAPUR. KARNATAKA.

IN PARTIAL FULFILLMENT OF THE REQUIREMENTS FOR THE DEGREE OF

MASTER OF DEGREE

IN

RADIO-DIAGNOSIS & IMAGING

Under the guidance of

DR. R. C. PATTANSHETTI M.B.B.S M.D.,

PROFESSOR,

DEPARTMENT OF RADIO-DIAGNOSIS & IMAGING

BLDEA'S

SHRI B. M. PATIL MEDICAL COLLEGE, HOSPITAL & RESEARCH CENTRE.

VIJAYAPUR – 586103

2016

B.L.D.E. UNIVERSITY'S

SHRI B. M. PATIL MEDICAL COLLEGE, HOSPITAL & RESEARCH CENTRE, VIJAYAPUR

DECLARATION BY THE CANDIDATE

I, **DR. PUNEET SHIRBUR,** hereby declare that this dissertation entitled **" DIFFUSION WEIGHTED MAGNETIC RESONANCE IMAGING FEATURES OF INTRACRANIAL LESIONS"** is a bonafide and genuine research work carried out by me under the guidance of **Dr. R. C. PATTANSHETTI** **M.D.,** Professor, Department of Radiodiagnosis, B.L.D.E.U's Shri B. M. Patil Medical College Hospital and Research Centre, Vijayapur.

Date:

Place: Vijayapur

Dr. PUNEET SHIRBUR

Post Graduate Student,

Department of Radiodiagnosis,

B.L.D.E.U's Shri B. M. Patil Medical College, Hospital & Research Centre,

Vijayapur

B.L.D.E. UNIVERSITY'S

SHRI B. M. PATIL MEDICAL COLLEGE, HOSPITAL

& RESEARCH CENTRE, VIJAYAPUR

CERTIFICATE BY THE GUIDE

This to certify that the dissertation entitled " **DIFFUSION WEIGHTED MAGNETIC RESONANCE IMAGING FEATURES OF INTRACRANIAL LESIONS"** is a bonafide research work done by **Dr. PUNEET SHIRBUR**, under my overall supervision and guidance, in partial fulfillment of the requirements for the degree of M. D. in Radiodiagnosis.

Date:

Place: Vijayapur

Dr. R. C. PATTANSHETTI M.D

Professor,

Department of Radiodiagnosis,

B.L.D.E.U's Shri B. M. Patil Medical College, Hospital & Research Centre, Vijayapur

B.L.D.E. UNIVERSITY'S

SHRI B. M. PATIL MEDICAL COLLEGE, HOSPITAL & RESEARCH CENTRE, VIJAYAPUR

ENDORSEMENT BY THE HEAD OF DEPARTMENT

This to certify that the dissertation entitled **"DIFFUSION WEIGHTED MAGNETIC RESONANCE IMAGING FEATURES OF INTRACRANIAL LESIONS"** is a bonafide research work done by **Dr. PUNEET SHIRBUR** under the guidance of **Dr. R. C. PATTANSHETTI** M.D., Professor, Department of Radiodiagnosis at B.L.D.E.U's Shri B. M. Patil Medical College Hospital and Research Centre, Vijayapur.

Date:

Place: Vijayapur

DR. BHUSHAN N. LAKHKAR M.D.
Professor & HOD,
Department of Radiodiagnosis,
B.L.D.E.U's Shri B. M. Patil Medical College, Hospital & Research Centre,
Vijayapur

B.L.D.E. UNIVERSITY'S

SHRI B. M. PATIL MEDICAL COLLEGE, HOSPITAL & RESEARCH CENTRE, VIJAYAPUR

ENDORSEMENT BY THE PRINCIPAL

This to certify that the dissertation entitled **"DIFFUSION WEIGHTED MAGNETIC RESONANCE IMAGING FEATURES OF INTRACRANIAL LESIONS"** is a bonafide research work done by **Dr. PUNEET SHIRBUR.** under the guidance of **Dr., R. C. PATTANSHETTI M.D.,** Professor, Department of Radiodiagnosis at B.L.D.E.U's Shri B. M. Patil Medical College Hospital and Research Centre, Vijayapur.

Date:

Place: Vijayapur.

DR. M. S. BIRADAR M.D.
Principal,
B.L.D.E.U's Shri B. M. Patil Medical College, Hospital & Research Centre,
Vijayapur.

B.L.D.E. UNIVERSITY'S

SHRI B. M. PATIL MEDICAL COLLEGE, HOSPITAL

& RESEARCH CENTRE, VIJAYAPUR

COPYRIGHT

DECLARATION BY THE CANDIDATE

I hereby declare that the B.L.D.E. UNIVERSITY, VIJAYAPUR, Karnataka shall have the rights to preserve, use and disseminate this dissertation/thesis in print or electronic format for academic/research purposes.

Date:
Place: Vijayapur

Dr. PUNEET SHIRBUR
Post Graduate Student,
Department of Radiodiagnosis,
B.L.D.E.U's Shri B. M. Patil Medical College, Hospital & Research Centre,
Vijayapur.

ACKNOWLEDGEMENT

This piece of work has been accomplished with the grace of almighty God. It gives me immense pleasure to express my heartfelt gratitude to all. I dedicate this page to each and everyone who has helped me to explore the expanses of knowledge.

I express my profound gratitude and sincere thanks to my guide, ***Dr. R.C. Pattanshetti*** *Professor, Department of Radio-diagnosis & imaging, B.L.D.E.U's Shri B. M. Patil Medical College, Vijayapur, for his constant and unfailing support, professional insight, valuable suggestions, motivation and exemplary guidance to carry out and complete this dissertation. I am deeply grateful to him for providing me necessary facilities and excellent supervision to complete this work.*

I offer my sincere thanks to ***Dr. M. S. Biradar****M.D.* *, Principal, B.L.D.E.U's Shri B. M. Patil Medical College, Vijayapur, for his support and inspiration.*

My sincere thanks to our Medical Superintendent ***Dr. VIJAYKUMAR*** *for his support and inspiration.*

I am deeply indebted and grateful to my professor ***Dr. Bhushan Lakhkar*** *M.D.,* *and* ***Dr. B R Dhamangoankar*** *M.D.,* *Department of, B.L.D.E.U's Shri B. M. Patil Medical College, Vijayapur, who with their valuable suggestions and constant guidance supported me throughout the preparation of this dissertation work.*

My thanks to ***Dr. Praveen M M*** *M.D.,* ***Dr S. V Patil****M.D..,* ***Dr. Satish Patil*** *M.D.,* ***Dr. Bhushita Lakhkar*** *M.D,.* *Assistant professors and* ***DR. M.M Patil*** *DMRD,* ***Dr. Vishal N.S*** *DNB.,* *Senior Resident, Department of Radio-diagnosis, B.L.D.E.U's Shri B. M. Patil Medical College, Vijayapur, for their valuable suggestions and encouragement which have definitely helped me improve my research work.*

I acknowledge my gratitude to ***Dr. Jonna Uday Bhaskar, Dr. Shivendra Chaudhary*** and ***Dr. Masudi Sheetal,*** *Postgraduate colleagues, Department of radio-*

diagnosis, B.L.D.E.U's Shri B. M. Patil Medical College, Vijayapur, for his support, advice and help in data collection.

I also thank all my seniors ***Dr. Narendra***, ***Dr. Sanjay***, ***Dr.Chaitra***, ***Dr.Sachin, and Dr.Vinod,*** *my juniors* ***Dr.Suresh, Dr Nandish, Dr. Naveen, Dr.Sourabh, Dr. Rohni, Dr. Parth, Dr. Holebasu and Dr.Avinash*** *for their co-operation during the preparation of this dissertation.*

I thank ***Mrs. Vijaya Soraganvi*** *statistician for her masterly guidance and statistical analysis. I sincerely acknowledge the support and kindness shown towards me by all the staff of Central Library, Shri B. M. Patil Medical College, Vijaaypur, at all times.*

I am thankful to all the Technical and non-teaching Staff of the Department of Ophthalmology, B.L.D.E.U's Shri B. M. Patil Medical College, Vijayapur for their co-operation.

I am deeply indebted to my beloved parents ***Dr. (Col) S.N Shirbur and Mrs. Jaya Shirbur*** *for their encouragement, support, blessings and sacrifices, which helped me to complete this dissertation.*

I thank ***Preeti Net zone***, *for their meticulous computerized layout of this dissertation.*

Last but not the least, my sincere thanks to all the patients of this study for their cooperation without which this study would not have been possible.

Date- ***Dr. PUNEET SHIRBUR***

Place:

LIST OF ABBREVIATIONS

ACA	-	Anterior Cerebral Artery
ADC	-	Apparent Diffusion Coefficient
CSF	-	Cerebro Spinal Fluid
CPA	-	Cerebello Pontine Angle
CT	-	Computed Tomography
DW	-	Diffusion Weighted
DWI	-	Diffusion Weighted Image
EPI	-	Echo Planar Image
FLAIR	-	Fluid Attenuation Inversion Recovery
FOV	-	Field of View
GBM	-	Glioblastoma Multiforme
HII	-	Hypoxic Ischemic Injury
MCA	-	Middle Cerebral Artery
MR	-	Magnetic Resonance
MRI	-	Magnetic Resonance Imaging
NCC	-	Neurocysticercosis
PCA	-	Posterior Cerebral Artery
PRES	-	Posterior Reversible Encephalopathy Syndrome
TIA	-	Transient Ischemic Attach
TE	-	Time of Echo,
TR	-	Time of Repetition
T1W	-	T1 Weighted,
T2W	-	T2 Weighted

ABSTRACT

Diffusion weighted imaging (DWI) is a specialized magnetic resonance imaging technique that depends on the random movement of water molecules within and between the intracellular and extracellular spaces. Regions with restricted mobility of water molecules yield a greater DW – MRI signal and appear bright. In apparent diffusion coefficient (ADC) images, regions that contain high water mobility appear bright.

Purpose:

The objectives of the study were to describe the imaging characteristics of intra cranial lesions on DWI and to compare these features with ADC and T2W images.

Materials and methods:

A descriptive MR study was undertaken in 72 patients detected to have intracranial lesions on DW MRI of the brain in BLDEU's Shri B.M Patil Medical College between October 2013 to July 2015. In all these patients the DWI findings were noted and correlated with ADC and T2 FLAIR images. All the MRI scans in this study were performed using 1.5 T MRI scanner (Philips Achieva).

Results:

In this study all cases (100%) of acute infarcts showed true diffusion restriction. 3 (15.78%) of acute infarcts showed no signal change on T2W images. The rest were hyperintense on T2WI. 1(33%) of subacute infarcts and none of the chronic infarcts showed diffusion restriction. All cases of subacute and chronic infarcts were hyperintense on T2WI. All 3 (100%) of the HII showed restricted diffusion while only 2 (66.66%) of them showed abnormal signal on T2WI.

All cases of abscesses showed diffusion restriction. The cystic or necrotic component of none of the tumors seen in this study showed true diffusion restriction. Extradural empyema showed restricted diffusion.

2 (50%) of cases of glioblastoma multiforme showed true restricted diffusion while none of the low grade gliomas or anaplastic astrocytomas showed diffusion restriction. Diffusion restriction was also noted in 75% of medulloblastomas and 50% of lymphomas.

Among extra axial tumors, 3 (60%) of meningiomas showed diffusion restriction. All cases of arachnoid cysts showed low signal on DWI while epidermoid cysts showed restricted diffusion.

Demyelination and PRES did not show restricted diffusion.

Conclusion:

DWI is a highly sensitive technique in the detection of acute infarcts and in characterizing infarcts as acute, subacute and chronic. DWI is a sensitive modality for detecting HII and shows the extent of involvement better than T2WI. Presence of diffusion restriction is a useful method of differentiating abscesses from necrotic or cystic neoplasms. Restricted diffusion may be a feature of high grade gliomas and may help in their grading. Highly cellular tumors such as lymphomas, medulloblastomas and meningiomas may show restricted diffusion. Arachnoid cysts can be differentiated from epidermoid cysts by the presence of low signal on DWI. PRES and demyelination do no show restricted diffusion probably due to lack of cytotoxic edema.

TABLE OF CONTENTS

LIST OF TABLES

LIST OF CHARTS

LIST OF FIGURES

INTRODUCTION

Diffusion weighted imaging is a technique that assesses local environment at the cellular level to determine changes in the random movement of water protons. Restricted diffusion appears as an area of increased signal on DWI and reduced signal on ADC images

It helps in detection of acute cerebral infarcts, (which constitute about 600 cases referred for MRI to our department per year) which occurs as a result of anoxic injury to the cell membrane. This results in reduced movement of water molecules between extra and intracellular compartments. Thus the earliest magnetic resonance imaging feature of stroke is hyperintensity on DWI with reduced signal on ADC. DWI and ADC intensity vary with the age of the ischemic stroke, a fact that can affect the analysis of clinical cases. Thus DWI in correlation with other sequences (like ADC) helps in early detection of acute infarct, at a stage when initiation of treatment can salvage the penumbra.

While DWI is mostly used to identify infarcts, other processes that interfere with or restrict the movement of water can cause notable changes on DWI, including neoplastic lesions, encephalitis, pyogenic abscesses and occasionally demyelinating disease.

Water diffusivity in the extracellular space is inversely related to the constituents of intracellular space; cells with a high nucleus to cytoplasm ratio and tissues with high cellularity cause increased volume of intracellular space, thus resulting in restriction of diffusion. Thus reduced diffusion can be seen in highly cellular tumors such as lymphoma, meningioma and glioblastoma.

Hence DWI in along with ADC can also be used to grade the cellularity of tumors, which in turn influences the treatment choices.

One of its main indications is also to differentiate between abscess (enhancing centre) and necrotic tumors (non-enhancing centre).

Conventional MR imaging and clinical findings might be non-specific in cases of herpes encephalitis. DW image shows high signal in the lesions with usually decreased ADC values representing cytotoxic edema and rarely higher ADC values representing vasogenic edema. Thus it increases the diagnostic accuracy when combined with other sequences.

Likewise DWI can be used to differentiate Creutzfeld-Jacob disease from infarct.

Multiple sclerosis is the most common demyelinating disease. DWI may improve lesion detection when combined with standard T2-weighted techniques. It also helps characterize lesion as acute and chronic

DWI is also an effective way of differentiating an arachnoid cyst from epidermoid tumors.

Hence DWI has a wide range of applications in the evaluation of intracranial pathological conditions. It provides a specific diagnosis in few situations, and adds to the information provided by conventional sequences in many others. It is in this backdrop, that we propose to do this study to understand the appearances of various intracranial lesions on diffusion weighted images and to help in follow up of the lesions . To understand the range of appearances of various lesions on DWI and ADC, we proposed to study 72 positive patients referred to our department. The signal characteristics of these lesions on ADC images and T2 FLAIR images will also be described.

OBJECTIVES

The objectives of the dissertation titled “Diffusion Weighted Magnetic Resonance Imaging Features on Intracranial Lesions” are as follows;

1. To describe the features of intracranial lesions on diffusion weighted imaging.
2. To compare the diffusion weighted imaging features of these lesions with ADC and T2 FLAIR images so as to help differentiate among them.

HISTORICAL PERSPECTIVE

Magnetic resonance imaging (MRI) was introduced into clinical medicine in 1981, and in short time since then it has assumed a role of unparallel importance in diagnostic imaging. Over the past 15 years MRI has emerged from the research laboratory to take its place as a premier imaging modality. [12] Magnetic resonance is a phenomenon involving magnetic fields and radio frequency (RF) electromagnetic waves. It was discovered in 1946 independently by Bloch and co-workers at Stanford and by Purcell at Harvard. (12,13)

In 1971, Raymond Damadian reported on the capability of NMR spectroscopy to differentiate between healthy and cancerous tissues. In 1973, Paul Lauterber developed and produced the first MRI image using capillary tubes of water and D2O. [14]

In 1976, Damadian and his colleagues produced the first MRI image of a live animal. The following year the first human image, depicting a crude representation of the thorax at the T8 level, was published by Damadian and his co-workers. Moore and Hinshaw produced the first recognizable images of the human brain. [14] MRI can produce images with excellent contrast between soft tissues and a high spatial resolution in every direction. MRI has been a useful tool for analytical chemistry and biochemistry, thanks to the discovery of chemical shift. [15,16]

The first measurements of diffusivity of water were made as early as in 1950s. In a series of classic experiments Carr and Purcell measured NMR self diffusion coefficient of water and other solvents using spin echo discovered by Hahn. [13] They showed that incoherent (diffusive) motion reduces the amplitude of NMR spin echo that is proportional to the diffusivity. Their conceptual framework is the basis of modern diffusion imaging techniques. [17]

In 1956, Torrey explicitly incorporated diffusion of magnetization in the Bloch equations and showed how it leads to additional attenuation in the NMR signal. The next key innovation in the evolution of NMR diffusion measurement was the development and use of pulsed field gradient methods.

Using their new pulsed gradient sequence, Stejskal and Tanner extended the findings of Carr and Purcell, showing that uniformly translating spins produce a net phase shift that is proportional to their velocity and the diffusing spins produce no net phase shift but a change in the height and width of phase distribution. [18]

PHYSICS AND TECHNIQUE OF DIFFUSION WEIGHTED IMAGING

The physics of diffusion weighted imaging

Diffusion weighted imaging is a relatively newer technique that enables visualization of the inherent directionality in the brain and provides an additional contrast based on the movement of water molecules. It is a technique that can characterize water diffusion properties at each picture element of an image. [19]

Physics of water diffusion

Molecular diffusion, or Brownian motion, was first formally described by Einstein in 1905. [20] Diffusion is the random motion of tissue water molecules. Tissue water molecules can diffuse randomly, however various intra and extracellular as well as micro and macro barriers influence diffusion. [16,21]

When molecules are agitated by thermal energy alone (i.e., when molecular displacement takes place through the process of diffusion), the displacement distribution is centered. This means that the average or net displacement of the molecular population is zero. This can be represented by a histogram. Displacement ‘r’ is plotted on X axis and probability ‘n/N’ is platted on Y axis. Probability refers to the proportion of molecules that are likely to undergo displacement by a distance ‘r’.

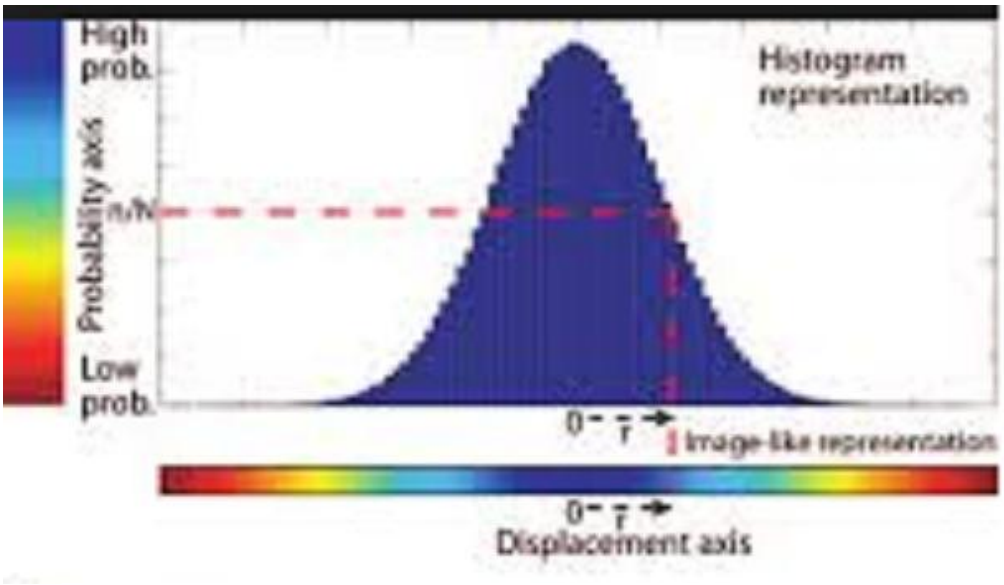

Figure 1: Probability v/s displacement graph - Diffusion

For each displacement distance r (x-axis) there is a corresponding probability n/N (y-axis), which is the proportion of molecules within a voxel that were displaced that distance within a time interval Δ (the duration of the diffusion experiment). The top of the histogram is centered on zero, indicating that most molecules had the same position at t = 0 and t = Δ. The proportion of molecules that traveled the given distance r is indicated by the dotted red line. The horizontal color bar, in which blue signifies a high probability and red a low probability of displacement, shows the same Gaussian distribution.

Factors other than heat also may contribute to molecular displacement. For example, a pressure gradient may affect molecular displacement. Such a setting produces a very different displacement distribution, in which the histogram is zero everywhere except in the position r, which has the value N/N = 1 because all the molecules have been displaced the same distance. This type of displacement is called flux. In an ideal setting with no turbulence and no friction, all molecules undergo the same non zero displacement ‘r’.

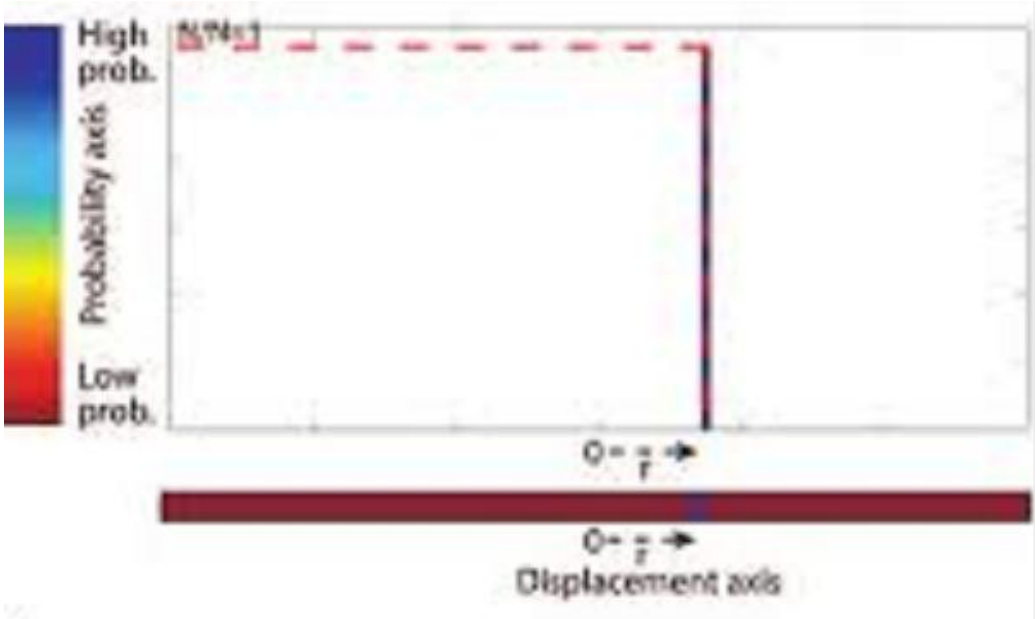

Figure 2 Probability v/s Displacement Graph - Flux

Biological tissues are highly heterogeneous media that consist of various compartments and barriers of different diffusivities. The movement of water molecules during diffusion driven random displacement is impeded by compartmental boundaries and other molecular obstacles in such a way that the actual diffusion distance is reduced compared with that expected in unrestricted diffusion.

A defining characteristic of neuronal tissue is its fibrillar structure. Neuronal tissue consists of tightly packed and coherently aligned axons that are surrounded by glial cells and that often are organized in bundles. As a result, the micrometric movements of water molecules are hindered to a greater extent in a direction perpendicular to the axonal orientation than parallel to it. Consequently, molecular displacement parallel to the fiber typically is greater than that perpendicular to it. [20]

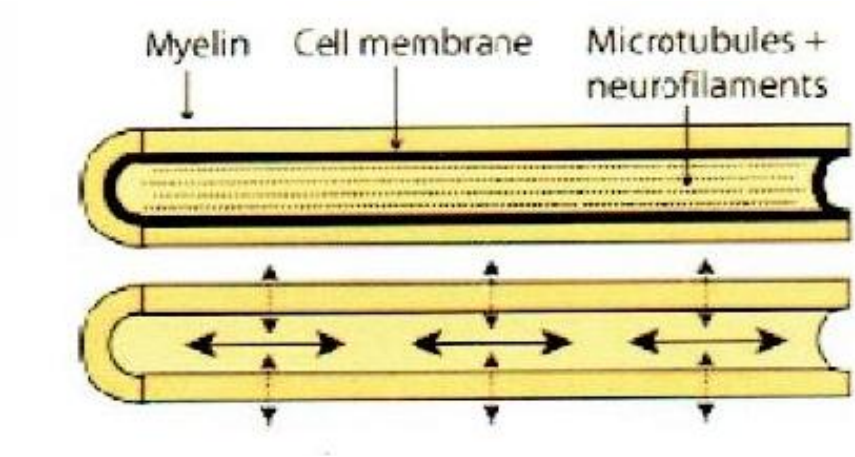

Fig 3 Anisotropic diffusion: Cell Membrane and Myelin

Acquiring diffusion weighted image

The basic principle of diffusion imaging is that the small random of the molecules results in a Gaussian distribution of phases. [13] The effect of these variations is enhanced by using a T2-weighted SE, gradient-echo, or echo-planar technique and applying strong gradients. The ability of these special pulse sequences to depict diffusion depends on the strength and duration of the diffusion gradients and on the direction in which they are applied. Diffusion is independent of the relaxation times and thus adds another factor to contrast. [21]

A typical Stejskal Tanner sequence uses two strong gradient pulses that allow controlled diffusion weighting, according to the following equation:

$S = S_0 e^{-bD}$

Where

S = Measured signal

S_0 = Signal without diffusion gradients

b = b factor

D = Diffusion coefficient

Its characteristic features are two strong symmetrical gradient lobes placed on either side of the 180^0 refocusing pulse in a spin echo sequence. [18] These symmetrical gradient lobes have the sole purpose of enhancing dephasing of spins, thereby accelerating the intravoxel incoherent motion signal loss.

The first of these pulses results in dephasing of the nuclear spins of the molecules affected by the B gradient (similar to the effect of T2 relaxation). The strength of this magnetic field on the hydrogen nuclei in water is partially based on their position in space. After the 180° echo pulse occurs, the second magnetic pulse gradient is applied. [22] This matching pulse acts to rephrase the nuclear spins, preserving the signal of the echo. However, if the nuclei in question have moved since the dephasing pulse, the rephrasing process will be incomplete, resulting in signal loss. Differences in signal intensity due to incomplete spin rephrasing form the basis of the DW image. [23]

Dephasing is proportional to the square of the time (diffusion time) during which the gradients are switched on and the strength of the applied gradient field. Therefore, the use of high field gradient systems with faster and more sensitive sequences, make diffusion weighting more feasible.

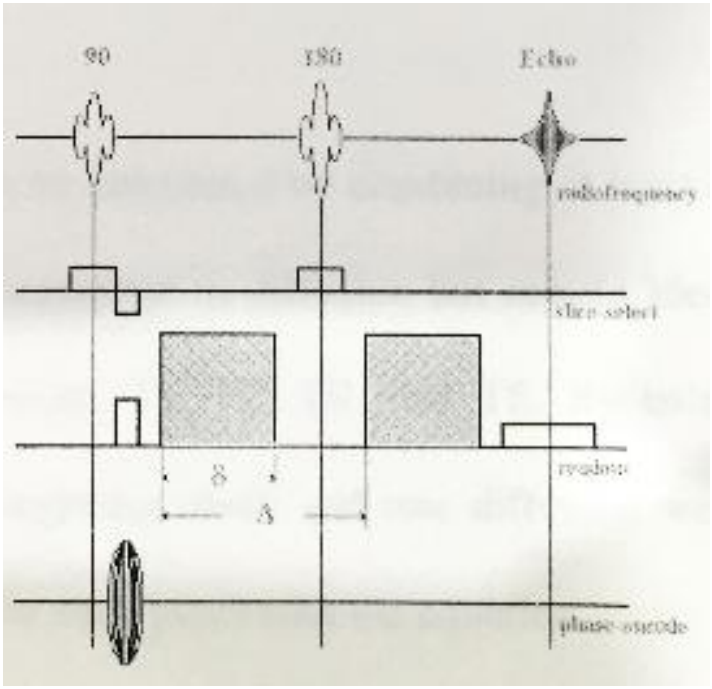

Fig 4 Stejskal Tanner sequence

The degree of diffusion weighting correlates with the strength of the diffusion gradients, characterized by the b-value, which is a function of the gradient related parameters; strength, duration and the period between diffusion gradients. [18,24]

Figure 3.5 Equation of Diffusion Weighting

b factor = ¥²G²¢² (a - ¢/3)

Where

γ = 42 MHz/tesla (proton gyromagnetic ratio)

G = Strength of the diffusion gradient pulses

δ = Duration of the diffusion gradient pulses

Δ = Time between diffusion gradient RF pulses

The signal intensity on diffusion-weighted images also depends on the spin density, T1, T2, TR and TE. To eliminate these influences and obtain pure diffusion information, we can calculate diffusion coefficient images.

A diffusion image can be calculated by combining at least two diffusion-weighted images that are differently sensitized to diffusion but remain identical with respect to the other parameters, spin density, T1, T2, TR and TE. By using, for instance, the image S_0 without diffusion weighting (b=0) and one diffusion weighted image (b > 0), we can calculate a D value for each pixel with the equation.

$$D = -\frac{1}{b} \, In \, \frac{S}{S_0}$$

A parametric image containing these data is called a diffusion map or apparent diffusion image (ADC). The latter term emphasizes the fact that the D values obtained with this procedure depend on the experimental conditions (e.g., direction of the sensitizing gradient and diffusion time delta). [25, 26]

Image contrast in Diffusion Weighted Imaging

If a Voxel of tissue contains water that has no net movement in the 'x' direction, the two balanced gradients cancel each other out. The resultant signal intensity of that Voxel is equal to its intensity on an image obtained with the same sequence without the DW gradients.

However, if water molecules have a net movement in the 'x' direction (e.g., due to diffusion), they are subjected to the first gradient pulse at one 'x' location and the second pulse at a different 'x' location. The two gradients are no longer equal in magnitude and no longer cancel. The difference in gradient pulse magnitude is proportional to the net displacement in the 'x' direction that occurs between the two gradient pulses, and faster moving water protons undergo a larger net dephasing.

The resultant signal intensity of a Voxel of tissue containing moving protons is equal to its signal intensity on a T2-weighted image decreased by an amount related to the rate of diffusion.

The signal intensity (SI) of a Voxel of tissue is calculated as follows;

$S = S_0 e^{-bD}$

Where

S_0 is the signal intensity on the T2- weighted (or b=0 sec/mm^2) image

b is the diffusion sensitivity factor, and

D is the diffusion coefficient

The diffusion sensitivity factor 'b' for the diffusion weighted sequence is described as;

b = ¥² G² ¦² (a - ¦/3)

Where

γ is the gyromagnetic ratio

G is the magnitude of

The width of, and

Δ the time between the two balanced DW gradient pulses

Apparent diffusion coefficient (ADC)

According to Fick's law, true diffusion is the net movement of molecules due to a concentration gradient. However MR imaging, cannot differentiate molecular motion due to concentration gradients from molecular motion due to pressure gradients, thermal gradients, or ionic interactions. Also, with MR imaging we do not correct for the volume fraction available or the increases in distance traveled due to tortuous pathways.

Therefore, when measuring molecular motion with DW imaging, only the apparent diffusion coefficient (ADC) can be calculated. Substituting 'ADC' for 'D', the signal intensity of a Voxel on a DW image is thus expressed as

$SI = SI_0 e^{-bD}$

With the original spin-echo T2-weighted sequence, even minor bulk patient motion was enough to obscure the much smaller molecular motion of diffusion. With the development of high-performance gradients, DW imaging can be performed with an echo-planar spin echo T2-weighted sequence. The use of echo-planar spin-echo T2-weighted sequence for DWI results in

1. Markedly decreased imaging time
2. Significant reduction in motion artifacts and
3. Increased sensitivity to signal changes due to molecular motion (diffusion)

As a result, it is clinically feasible to perform DW imaging

Other methods of performing DW-MRI without echoplanar gradients have also been developed. These include DW sequences based on a single-shot gradient and spin-echo or single-shot fast spin-echo techniques. [25, 26]

"line-scan" DW and spiral DW sequences have also been developed. [27]

Diffusion Anisotropy

In the brain, particularly in the white matter, diffusion is not isotropic (the same in all directions); it is anisotropic (varies in different directions). Diffusion of water is typically facilitated along the direction of the white matter fibers and is restricted in a direction perpendicular to it. The cause of the anisotropic nature of white matter is not completely understood. It is likely that in addition to axonal direction and myelination, other physiologic processes, such as axolemmic flow,

extracellular bulk flow, capillary blood flow, and intracellular streaming, may contribute to white matter anisotropy. [28, 29]

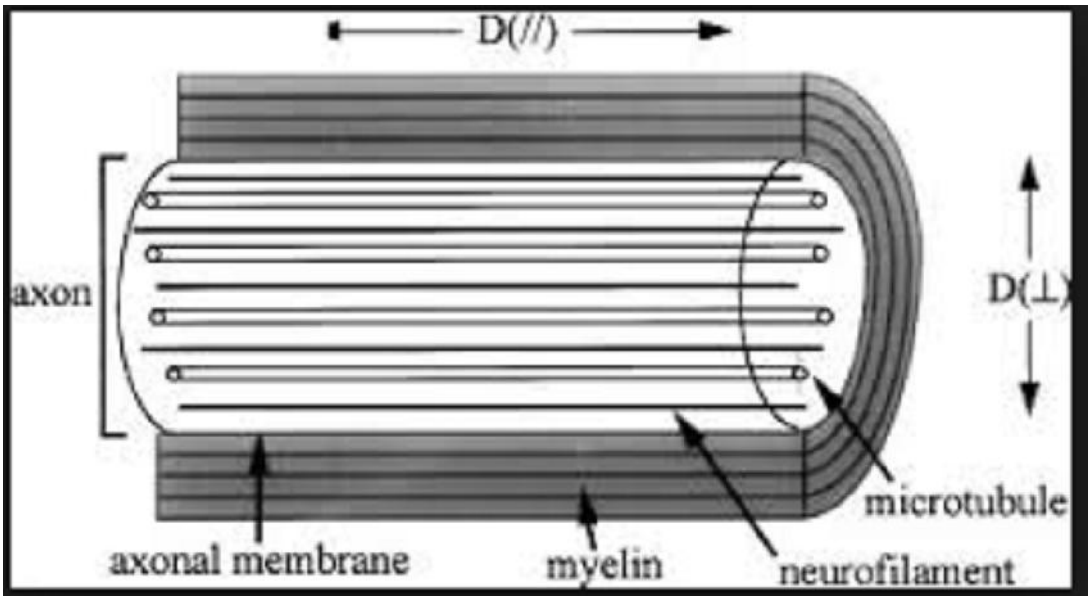

Fig 5 Factors contributing to anisotropic diffusion

The anisotropic nature of diffusion in the brain can be appreciated by comparing images obtained with DW gradients in three orthogonal directions (Fig 4).

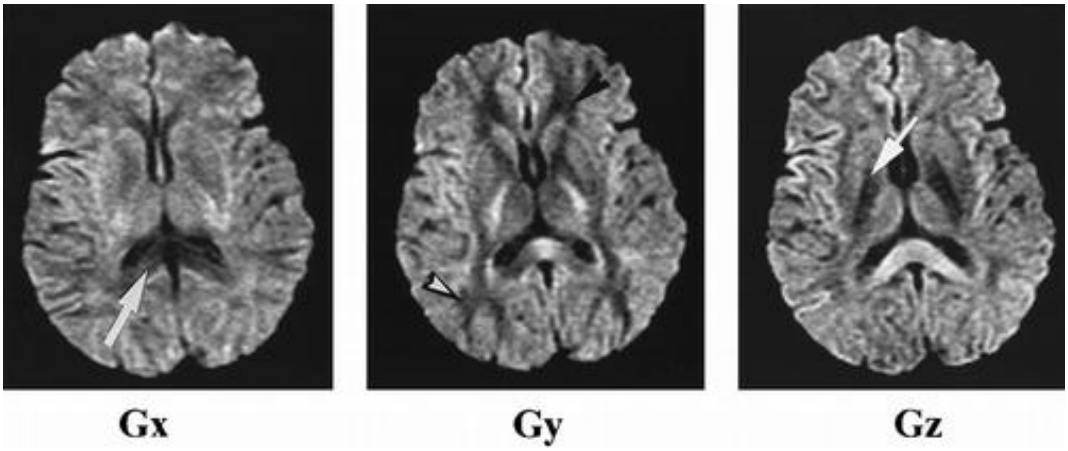

Fig 6 Diffusion Anisotropy within brain

Axial DW MR images with the diffusion gradient applied along the x (Gx, left), y (Gy, middle), and z (Gz, right) axes demonstrate anisotropy. The signal

intensity decreases when the white matter tracts run in the same direction as the DW gradient because water protons move preferentially in this direction. Note that the corpus callosum (arrow on left image) is hypointense when the gradient is applied in the x (right-to-left) direction, the frontal and posterior white matter(arrowheads) are hypointense when the gradient is applied in the y (anterior-to-posterior) direction, and the corticospinal tracts (arrow on right image) are hypointense when the gradient is applied in the z (superior-to-inferior) direction.

In each of the images, the signal intensity is equal to the signal intensity on echo-planar T2 weighted images decreased by an amount related to the rate of diffusion in the direction of the applied gradients. Images obtained with gradient pulses applied in one direction at a time are combined to create DW images or ADC images.

DW gradient pulses are applied in one direction at a time. The resultant image has information about both the direction and the magnitude of the ADC (Fig 4). To remove the effect of directional variance of diffusion due to white matter structure, ‘isotropic’ diffusion weighted images are calculated from three diffusion weighted images that are acquired with diffusion sensitization gradients applied in the ‘x’, ‘y’ and ‘z’ directions. The signal intensity of each voxel on the DWI is calculated as the cube root of the product of signal intensities of the voxel in each of these images.

.

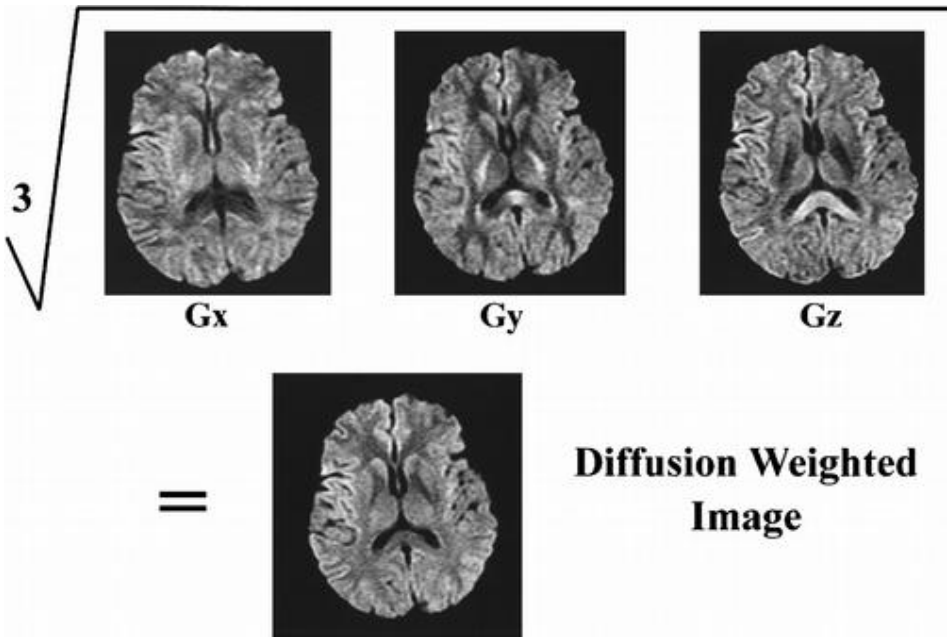

Fig 7 Calculation of signal intensity on an isotropic DW image

The signal intensities of the three transverse images (Gx, Gy, and Gz), each with a diffusion gradient applied in one of three orthogonal directions, are multiplied together. Here the DW gradients were applied along the x, y, and z axes. The signal intensity of the isotropic DW image (bottom) is essentially the cube root of the signal intensities of these three images multiplied together. Note that both T2-weighted contrast and the rate of diffusion contribute to the signal intensity of the isotropic DW image. Images displaying the magnitude of the ADC are used in clinical practice. [30]

Removal of T2 weighted contrast

It is important to understand that DW image has T2-weighted contrast as well as contrast due to differences in ADC. To remove the T2-weighted contrast, DW image can be divided by the echo-planar spin-echo T2-weighted (or b = 0 sec/mm^2) image to give an "exponential image". To remove the T2-weighted contrast in the isotropic transverse DW image, the axial DW image (DWI) is divided by the transverse echo-planar spin-echo T2-weighted (EP SET2) image. The resultant image

is called the exponential image because its signal intensity is exponentially related to the ADC. Alternatively, an ADC image, which is an image whose signal intensity is equal to the magnitude of the ADC, can be created.

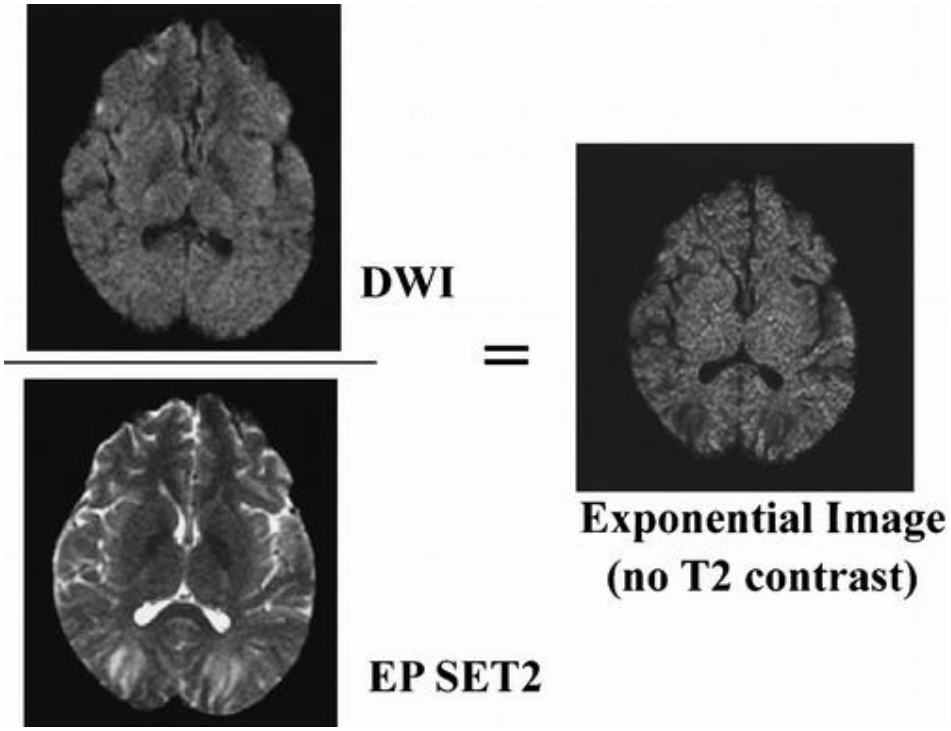

Fig 8 Removal of T2 contrast

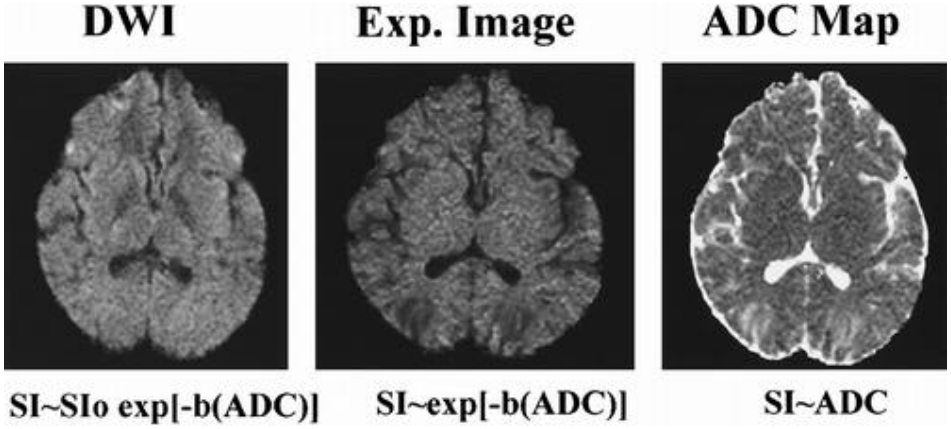

Fig 9 Creation of ADC map

One method of creating an ADC image is to mathematically manipulate the exponential (Exp.) image. Because the ADC values of gray and white matter are similar, typically there is no contrast between gray and white matter on the exponential image or ADC image. The contrast between gray and white matter seen on the DW image is due to T2-weighted contrast. This residual T2 component on the DW image makes it important to view either the exponential image or ADC image in conjunction with the DW image. [31]

Diffusion Weighted Image Artifacts

Numerous well know artifacts can affect DWI quality. Subject motion during the MR scan can cause Ghosting artifact of artifactual redistribution of the signal intensities within DWI. Rigid body motion, such as rotation and translation are the easiest to correct for, as they are involved applying a uniform phase offset to an entire image. This problem has been addressed by incorporating navigator echoes in the DWI pulse sequence. More pernicious is non-rigid body motion caused by eye movements, pulsating of the CSF, etc. These artifacts have not been completely eliminated but they can be mitigated by the use of fast DWI sequences and cardiac gating methodologies are now routinely utilized in the implementation of diffusion MR techniques in patients, such as in early stroke diagnosis and characterization.

The large, rapidly switched magnetic field produced by the gradient coils during the diffusion sequence induce eddy currents in the electrically conductive structures of the MR scanner, which in turn produces an additional unwanted, slowly decaying magnetic field. Two undesirable effects result:

i. The field gradient at the sample differs from prescribed field gradient thus causing a deviation from the prescribed b-matrix, and

ii. The slowly decaying field causes geometrical distortion of the DWWI. These artifacts can adversely affect diffusion imaging studies because the diffusion coefficient or diffusion tensor are generally calculated in each voxel from a multiplicity of the DWIs assuming that the prescribed gradients are the same as the gradients actually being applied to the tissue.

Uncompensated image distortion can lead to systemic errors in these estimated diffusion parameters. Unfortunately, single shot Echo-planar (EPI) acquisitions are quite susceptible to eddy current artifacts so correction schemes have to be used. One widely used strategy is to wrap each DWI to a complete template; another is to try to use a model of the effect of the eddy current on the phase map to correct it. Other investigators implement no EPI alternatives, such as line scan diffusion imaging (LDWI). [32]

Large discontinuities is the bulk magnetic susceptibility, such as those that occur at tissue air interfaces produces local magnetic field gradients which notorious for their contribution to image distortion particularly in EPI. In addition to the image distortion, susceptibility variations within the brain adversely affect DWIs because the additional local gradients act like diffusion gradients causing the b-matrix to be spatially varying. Fortunately, this affect appears to be limited to the volume of the brain adjacent to the sinuses.

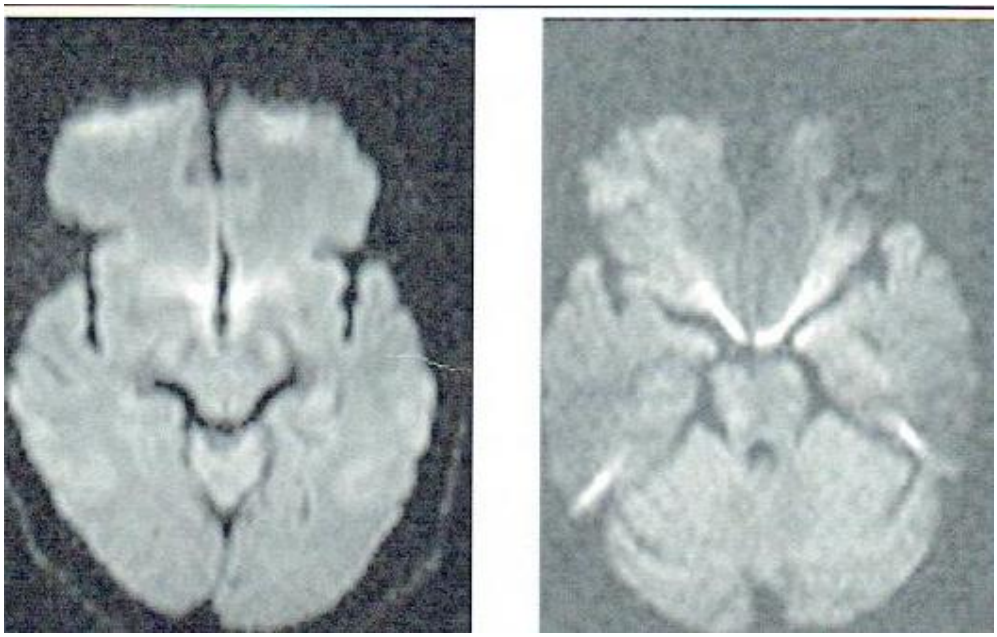

Fig 10 Susceptibility Artifact

While at low levels diffusion weighting the logarithm of the signal attenuation decreases linearly with increasing the b-value, background noise cause the DWI intensity to approach a baseline “noise factor” as one progressively increase the degree of diffusion weighting. Noise can introduce errors in the estimated diffusion coefficients as it makes isotropic media appear anisotropic, and anisotropic media appear more anisotropic.

Improper refocusing of RF pulses leads to additional signal loss. Background gradients can be present because of improper shimming. This leads to additional signal attenuation if not properly compensated for. Measuring background gradient directly and incorporating them explicitly in the formula can often remedy this problem. [33]

T2 shine through effect

The relative contributions of abnormal diffusion and the intrinsic T2 properties are difficult to determine on diffusion-weighted alone. A T2 hyperintense lesion can, in the absence of restricted diffusion, still appear hyperintense on DW images, a

phenomenon called “T2 shine-through”. The resultant hyperintense signal on diffusion-weighted images, which is attributable to the intrinsic T2 signal characteristics of the tissue, has been termed the T “shine-through” effect. T2 shine-through effect can be eradicated is by generating an ADC image that reflects only the diffusional properties of water and not the characteristics of the T2 signal. Therefore true restricted diffusion is defined as presence of hyperintensity on DWI and hypointensity on ADC images.

T2 washout

Refers to presence of isointense lesions on DWI i.e., normal DWI with increase in the apparent diffusion coefficient. This phenomenon resulting from a balance of T2 effects and increased water diffusibility has been term as T2 washout phenomenon. It is result of intravoxel dephasing related to the increased water diffusion in the vasogenic edema that washes out the inherent increased T2 signal intensity in the lesions. This phenomenon has been first decreased in PRES, through not unique of it, and can be seen in any pathological conditions. (34) A malignant mass lesion also causes significant mass effect and associated vasogenic edema which causes T2 washout phenomenon.

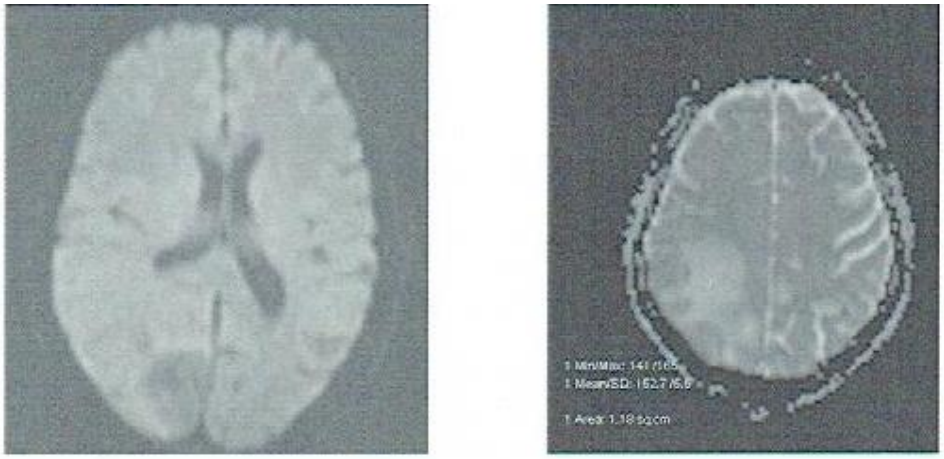

Fig 11 T2 washout

Diffusion/T2 blackout

The term diffusion blackout refers to hypointensity on T2, DWI and ADC image. This pitfall of susceptibility induced signal losses complicating ADC measurements in acute hematomas. T2 blackout effect can also be seen in Tumor calcification induced susceptibility effect. Thus T2 blackout effect is coronally of the T2 shine-through effect.

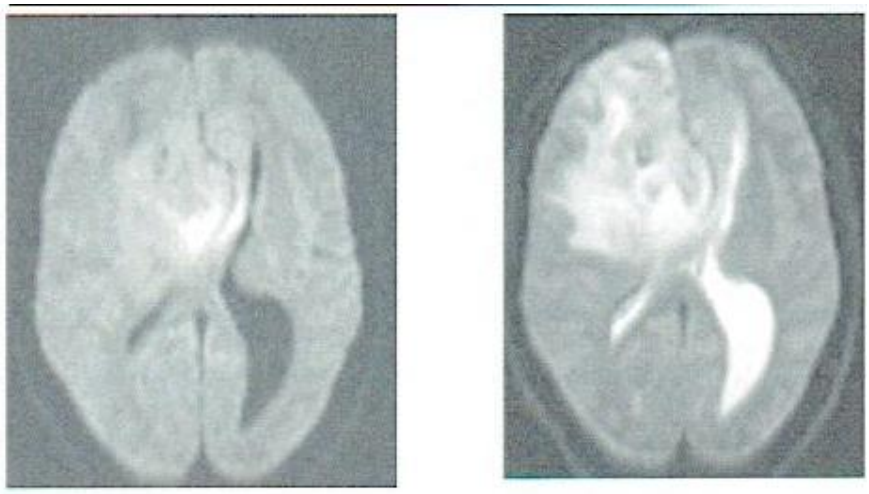

Fig 12 T2 blackout

Normal appearance of the brain on DWI

Normal gray matter is brighter than white matter on DWI. The contrast between gray and white matter seen is due to T2 weighted contrast. Isotropic DW imaging in adult brain often shows low signal intensity in the basal ganglia. This low signal is caused by normal iron deposition. The hypointensity on DW images of these areas is essentially related to T2 contrast. ADC images usually show the areas as iso-intense, but it can be hyper-or hypointense depending on the paramagnetic susceptibility artifact of iron deposition. [35]

The choroid plexus occasionally shows prominent hyperintensity on DW imaging associated with mild elevation of ADC. In these situations the ADC is often

higher than in which matter, but lower than in cerebrospinal fluid. The high DW signal is believed to represent gelatinous cystic changes o the choroid plexus, which can occur with age.

Many authors have evaluated the diffusion changes in the aging brain. They have found that there is minimal increase in the ADC values of aging brain. [36] Terry Chun et al [37], evaluated the diffusion changes in the aging brain. They found that the mean diffusion value of the human brain is nearly constant throughout most of adulthood. Mild increase in the ADC with age might be significant for individuals 60 years or older compared with younger subjects. Measurements from the periventricular white matter and thalamus obtained using ROIs showed an age-dependent increase in ADC of the periventricular white matter, but no changes in the thalamus.

Table: Normal apparent diffusion coefficient values

Tissue	ADC
Normal gray matter	$0.70 \pm 0.03 \times 10^{-3}$ mm^2/sec
Normal white matter	$0.75 \pm 0.03 \times 10^{-3}$ mm^2/sec
CSF	3×10^{-3} mm^2/sec

ADC in neonates and infants varies markedly within different areas of the brain and is higher in white matter (1.13×10^{-3} mm^2/sec) than in gray matter (1.02×10^{-3} mm^2/sec). ADC at birth is higher in subcortical white matter (1.88×10^{-3} mm^2/sec) than in both the anterior (1.30×10^{-3} mm^2/sec) and posterior limbs of the internal capsule (1.10×10^{-3} mm^2/sec). It is also higher in the cortex and the caudate nucleus (1.0×10^{-3} mm^2/sec) than in the thalamus and the lentiform nucleus ($1.20 \times 10^{-}$

^{3} mm^2/sec). With the exception of the cerebrospinal fluid (CSF), there is a trend of decreasing ADC with increasing maturation in most areas of the pediatric brain. [38, 39]

REVIEW OF LITERATURE

DWI applications in intracranial lesions

Diffusion weighted imaging provides image contrast that is dependent on the molecular motion of water, which may be substantially altered by disease. The normal random movement of water molecules is affected by various pathological conditions which alter the signal generated on DWI. Schaffer PW et al in diffusion weighted MR imaging of the brain, Radiology (November 2000) [(40)] suggested that these features can be used to identify and characterize the lesions. [(40)]

Ischemic stroke

Theory of restricted diffusion in acute stroke

Chien D et al in MR diffusion imaging of cerebral infarctions in humans (1992) [(41)] suggested that within minutes after the onset of ischemia, a profound restriction in water diffusion occurs in affected brain tissue. [(41)] The biophysical basis of this change is not completely clear. Mintorovitch et al, in Diffusion-weighted magnetic resonance imaging of acute focal cerebral ischemia;comparison of signal intensity with changes in brain water and Na+, K+ and ATP'ase activity (1994) [(42)] found that one likely important contributor to this change is cytotoxic edema. Cytotoxic edema is associated with a reduction in Na^+/K^+ adenosine triphosphatase activity without a significant increase in brain water. (42) Ischemia causes disruption of energy metabolism, leading to failure of the Na^+/K^+ adenosine triphosphatase pump and other ionic pumps. This leads to loss of ionic gradients and a net translocation of water from the extracellular to the intracellular compartment, where water mobility is relatively more restricted.

Schiuer G et al, in The repeatability of MR perfusion studies: A clinical study (1995) [(43)] found that there are additional factors with cellular swelling; there is a

reduction in the volume of extracellular space. [43] Proposed explanations are increased intracellular viscosity due to dissociation of microtubules and fragmentation of other cellular components or increased tortuosity of the intracellular space and decreased cytoplasmic mobility. The normal steady state function of these structures requires energy and uses adenosine triphosphate. Le Bihan D et al, in temperature mapping with MR imaging of molecular diffusion; application to hyperthermia (1989) [44] and Helpen J et al, in the effect of cell membrane water permeability on the apparent diffusion coefficient of water (1992) [45] found that other factors such as temperature [44] and cell membrane permeability [45] play a minor role in explaining the reduction in ADC in acutely ischemic tissue.

Time course of lesion evolution in acute stroke

Lutsep H et al, in Clinical utility of diffusion-weighted magnetic resonance imaging in the assessment of ischemic stroke (1997) [46] and Schwamm L et al, in Time course of lesion development in patients with acute stroke: serial diffusion and hemodynamic weighted magnetic resonance imaging (1998) [47] found that in adult humans restricted diffusion associated with acute ischemia is seen 30 minutes after a witnessed ictus. The ADC continues to decrease and is most reduced at 8-32 hours. The ADC remains markedly reduced for 3-5 days. This decreased diffusion is markedly hyperintense on DW images (which are generated with a combination of T2-weighted and DW imaging) and hypointense on ADC images. The ADC returns to baseline at 1-4 weeks. This most likely reflects persistence of cytotoxic edema (associated with decreased diffusion) and development of vasogenic edema and cell membrane disruption, leading to increased extracellular water (associated with increased diffusion). At this point, an infarction is usually mildly hyperintense due to the T2 component on the DW images and is isointense on the ADC images.

Thereafter, diffusion is elevated as a result of continued increase in extracellular water, tissue cavitation, and gliosis. This elevated diffusion is characterized by slight hypointensity, isointensity, or hyperintensity on the DW images (depending on the strength of the T2 and diffusion components) and increased signal intensity on ADC images. [46, 47]

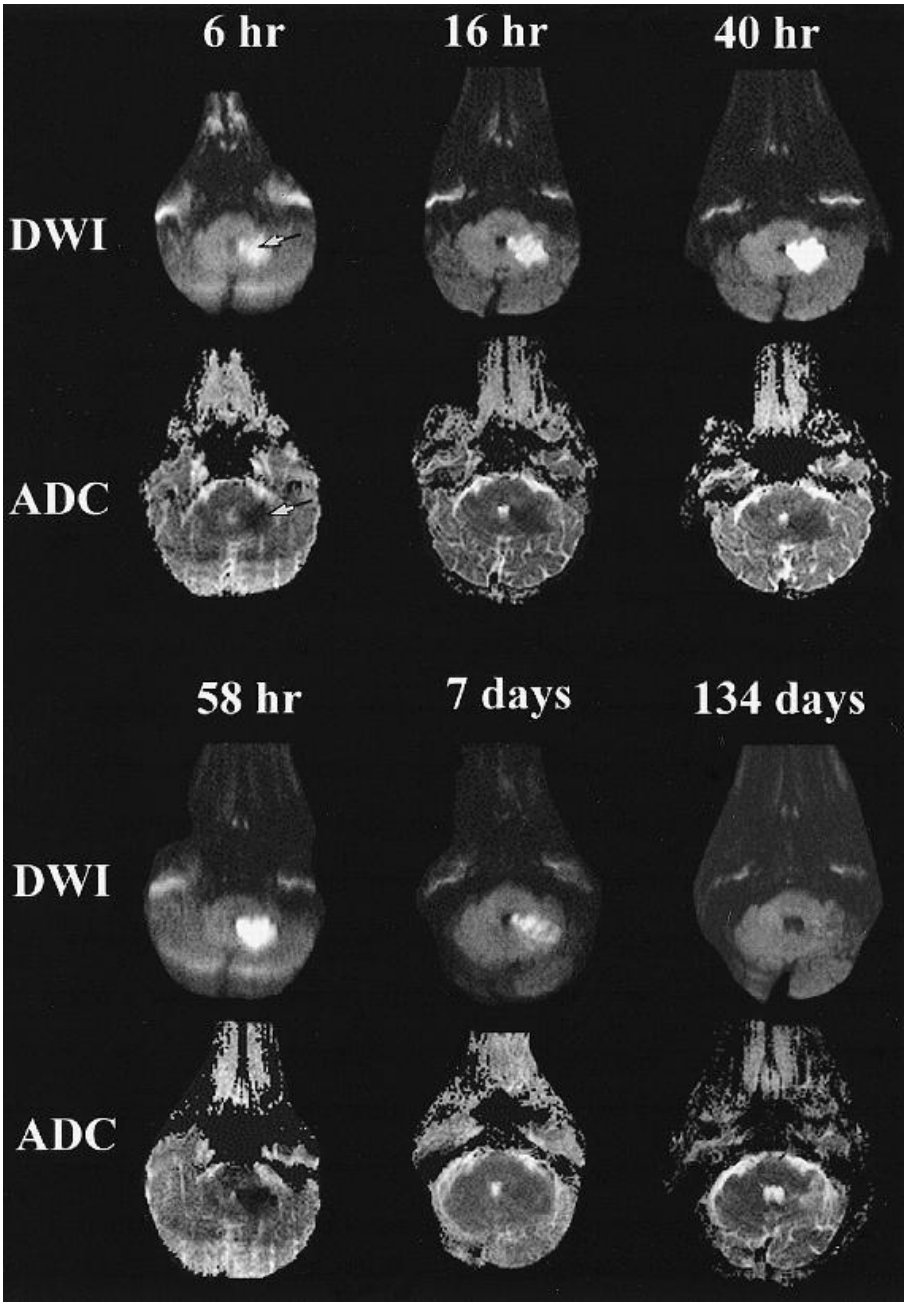

Fig 13 Time course of acute infarct

At 6 hours, the lesion (arrows) is hyperintense on the DW images and hypointense on the corresponding ADC image. The lesion becomes progressively more hyperintense on DW images, reaching its maximum hyperintensity at the 58-hour time point, when it also reaches its maximum hypointensity on ADC images. At 7 days, there is ongoing resolution of the lesion on both DW images and ADC images. By 134 days, there is subtle hypointensity on the DW image and hyperintensity on the ADC images.

Marks M et al, in Time course of lesion development in patients with acute stroke: serial diffusion and hemodynamic weighted magnetic resonance imaging (1999) [(48)] demonstrated that the time course does not always conform to the aforementioned outline. With early reperfusion, pseudonormalization (return to baseline of the ADC reduction associated with acute ischemic stroke) may occur at a much earlier time – as early as 1-2 days in humans given intravenous recombinant tissue plasminogen activator less than 3 hours after stroke onset. [(48)] Furthermore, Nagesh et al, in Time course of ADC changes in ischemic stroke: beyond the human eye (1998) [(49)], demonstrated that although the mean ADC of an ischemic lesion is depressed within 10 hours, different zones within an ischemic region may demonstrate low, pseudonormal, or elevated ADCs, variations, tissue characterized by an initial reduction in ADC nearly always undergoes infarction in humans.[(49)]

5.2.3 Reversibility of ischemic lesions on DW images

Schafer PW et al, in Diffusion weighted MR imaging of the brain (2000) [(40)] found that in humans, reversibility of ischemic lesions is rare. There is neither a threshold

time nor a threshold ADC for reversibility that has been established. Very few cases of reversibility of DWI changes in stroke have been reported. [40]

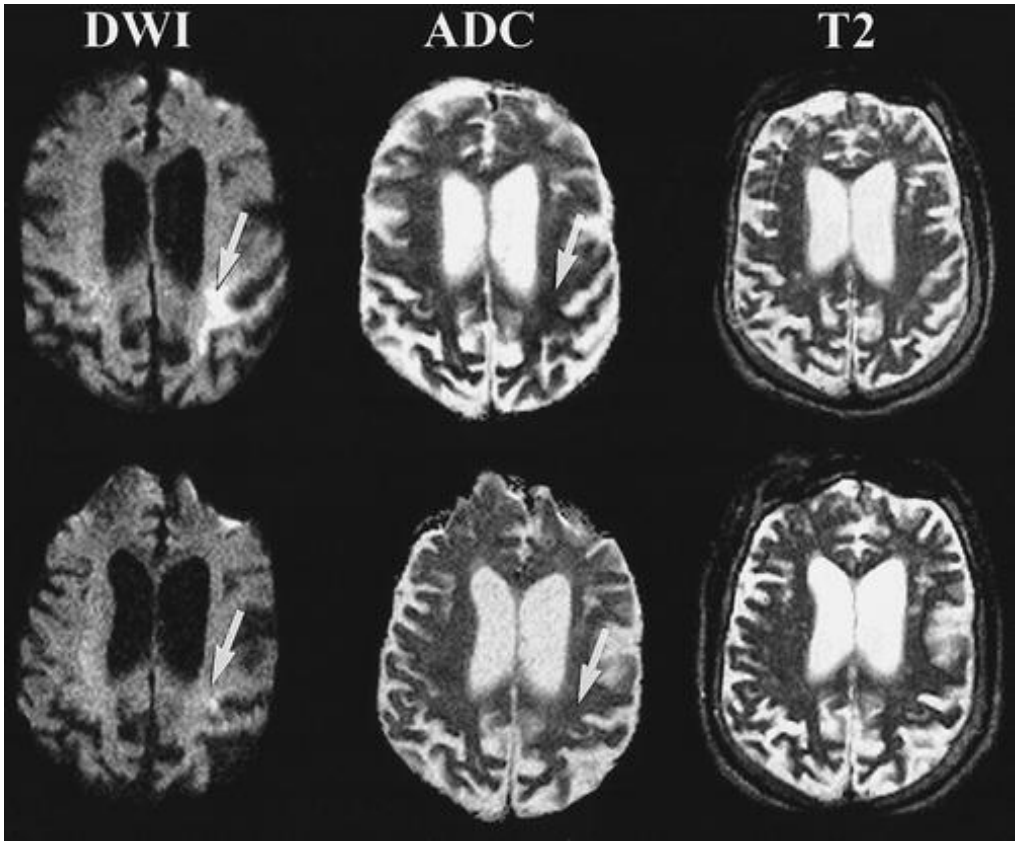

Fig 14 Reversibility of acute infarct

Top: Transverse DW image shows an area of hyperintensity (arrow) in the left posterior frontal and anterior parietal lobes. Top middle: of hypointensity (arrow) corresponding to this area is seen on the transverse ADC image (arrow). Top right: No definite abnormality is seen on the transverse fast spin-echo T2-weighted MR image. The patient was treated with intravenous recombinant tissue plasminogen activator, with resolution of the neurologic symptoms.

Follow-up images obtained 3 days later demonstrate near interval resolution of the abnormalities on the 2-hour DW image and ADC image. No definite lesion was identified on the follow-up T2-weighted image.

DW imaging reliability in acute stroke

Conventional computed tomography (CT) and MR imaging cannot be used to reliably detect infarction at the earliest time points. The detection of hypoattenuation on CT scans and hyperintensity on T2-weighte MR images requires an increase in tissue water. This was confirmed by Mohr J et al, in Magnetic resonance versus computed tomographic imaging in the acute stroke (1995) [(50)] who showed that for infarctions imaged within 6 hours after stroke onset, reported sensitivities are 38%-45% for CT and 18% - 46% for conventional MR imaging. For infarctions imaged within 24 hours, Bryan R et al. in Diagnosis of acute cerebral infarction: comparison of CT and MR imaging (1991) [(51)] reported a sensitivity of 58% for CT and 82% for conventional MR imaging in their study.

Gonzalez RJ et al. in Diffusion-weighted MR imaging: diagnostic accuracy in patients imaged within 6 hours of stroke symptom onset (1992) [(52)] and Lovblad K et al. in Clinical experience with diffusion-weighted MR in patients with acute stroke (1998) [(53)] showed through their studies that DW images are very sensitive and specific for the detection of hyperacute and acute infarctions, with a sensitivity of 80% - 100% and a specificity of 86% - 100%. A lesion with decreased diffusion is strongly correlated with irreversible infarction. However, acute neurologic deficits suggestive of stroke but without restricted diffusion are typically due to transient ischemic attack, peripheral vertigo, migraine, seizures, intracerebral hemorrhage, dementia, functional disorders, amyloid angiopathy , and metabolic disorders as seen by Gonzalez RJ et al,. (1992) [(52)] and Lovblad K et al. (1998) [(53)] in their studies. Although, after 24 hours, infarctions usually can be detected as hypoattenuating lesions on CT and hyperintense lesions on T2-weighted and FLAIR MR images, DW imaging is useful in this setting, as well. Older patients commonly have hyperintense

abnormalities on T2-weighted images that may be indistinguishable from acute lesions. However, acute infarctions are hyperintense on DW images and hypointense on ADC images, whereas chronic foci are usually isointense on DW images and hyperintense on ADC images due to elevated diffusion. This was substantiated by Singer M et al. in Diffusion-weighted MRI in acute subcortical infarction (1998) [(54)] in which there were indistinguishable acute and chronic white matter lesions on T2-weighted images in 69% of patients, the sensitivity and specificity of DW imaging for detection of acute subcortical infarction were 94.9% and 94.1% respectively.

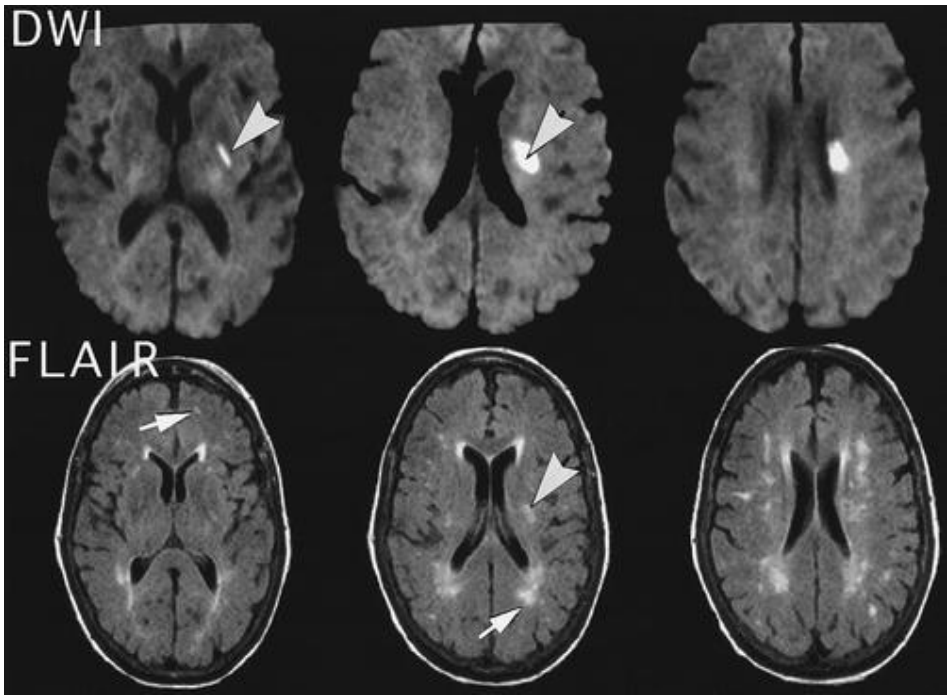

Fig 15 acute and chronic infarct – DWI and T2FLAIR

Top: Transverse DW images in the top row clearly demonstrate the acute infarction (arrowheads) in the putamen and corona radiate. Bottom: FLAIR images demonstrate multiple white matter lesions in which acute (arrowhead) and chronic lesions (arrows) cannot be differentiated.

Gonzalez RG et al. (1999) [(52)] and Lovbald K et al. (1998) [(53)] reported False-negative DW images in patients with very small lacunar brainstem or deep gray nuclei

infarction. Some of these lesions were seen on follow-up DW images, and others were presumed to be present on the basis of clinical deficits. False-negative DW images also occur in patients with regions of decreased perfusion (increased mean transit time and decreased relative cerebral blood flow), which are hyperintense on follow-up DW images; in other words these patients initially had regions characterized by ischemic but viable tissue that progressed to infarction. These findings stress the importance of obtaining early follow-up images in patients with normal DW images and persistent stroke-like deficits, so that infarctions or areas at risk for infarction are identified and treated as early as possible. [52, 53]

False-positive DW images have been reported in patients with a diagnosis other than acute infarction. These include cerebral abscess (with restricted diffusion on the basis of viscosity) and tumor (with restricted diffusion on the basis of dense cell packing). When these lesions are viewed on DW images in combination with other routine T1 and T2-weighted MR images, they can usually be differentiated from acute infarctions.

Correlation of DW MR imaging with clinical outcome

DW MR imaging findings may reflect the severity of clinical neurologic deficits and help predict clinical outcome. Statistically significant correlations between the acute DW MR lesion volume and both acute and chronic neurologic assessment results have been demonstrated by Schwamm L et al. in Time course of lesion development in patients with acute stroke: serial diffusion and hemodynamic weighted magnetic resonance imaging. (1998) [47] and Lovbald K et al. in Ischemic lesion volumes in acute stroke by diffusion-weighted magnetic resonance imaging correlation with clinical outcome (1997) [56]. They showed that this correlation is stronger in cases of cortical stroke and weaker in cases of penetrator artery stroke.

Lesion location likely explains the variance; for example, a lesion in a major white matter tract may produce a more profound neurologic deficit than would a cortical lesion of the same size. [47, 56]

In addition, Schwamm L et al. (1998) [47] and Everdingen KJ et al. in Diffusion-weighted magnetic resonance imaging in acute stroke (1998) [57] found a significant correlation between the acute ADC ratio (lesion ADC to normal contralateral brain ADC) and chronic neurologic assessment scale scores. [47, 57]

Transient ischemic attacks

Ay H et al. in Clinical and diffusion-weighted imaging characteristics of an identifiable subset of TIA patients with acute infarction (1999) [58] and Kidwell et al. in Diffusion MRI in patients with transient ischemic attacks (1999) [59] found that nearly 50% of patients with transient ischemic attacks have lesions characterized by restricted diffusion. [58, 59] These lesions are usually small (<15 mm diameter), are almost always in the clinically expected vascular territory, and are thought to represent markers of more widespread reversible ischemia. In the study by Kidwell et al. (1999) [59], 20% of the lesions were not seen at follow-up; the lesions could have been reversible or, owing to atrophy, too small to see on conventional MR images. The information obtained from DW MR imaging changed the suspected localization of an ischemic lesion, as well as the suspected etiologic mechanism, in more than one third of patients. [59] In the other study by Ay H et al. (1999) [58], statistically significant independent predictors for identification of these lesions on DW MR images included previous non-stereotypic transient ischemic attack, cortical syndrome, or an identified stroke mechanism, and the authors suggested an increased stroke risk in patients with these lesions. Early identification of patients with transient

ischemic attack with increased risk of stroke and better identification of etiologic mechanisms is changing acute management and may affect patient outcome. [58]

Lesions with reversible vasogenic edema

Syndromes with potentially reversible vasogenic edema include eclampsia, hypertensive encephalopathy, cyclosporine toxicity, other posterior leukoencephalopathies, venous thrombosis and human immunodeficiency virus encephalopathy. Patients with these syndromes frequently present with neurologic deficits that are suggestive of acute ischemic stroke or with neurologic features such as headache or seizure that are suggestive of vasogenic edema, but ischemic stroke is still a strong diagnostic consideration. Conventional MR imaging cannot help differentiate vasogenic edema from the cytotoxic edema associated with acute infarction. Cytotoxic edema produces high signal intensity in gray and/or white matter on T2-weighted images. Although vasogenic edema on T2-weighted images typically produces high signal intensity in white matter, the hyperintensity can involve adjacent gray matter. Consequently, posterior leukoencephalopathy can sometimes mimic infarction of the posterior cerebral artery. Human immunodeficiency virus encephalopathy can produce lesions in a variety of distributions, some of which have a manifestation similar to that of arterial infarction. Deep venous thrombosis can produce bilateral thalamic hyperintensity that is indistinguishable from “top of the basilar” syndrome arterial infarction.

DW MR imaging can be used to reliably distinguish vasogenic from cytotoxic edema. Tien R et al. in MR imaging of high grade gliomas: value of difffusion-weighted echo-planar pulse sequences (1994) [60] and Schwartz R et al. in Diffusion-weighted MR imaging in hypertensive encephalopathy: clues to pathogenesis (1998) [61] found that while cytotoxic edema is characterized by restricted diffusion,

vasogenic edema is characterized by elevated diffusion due to a relative increase in water in the extracellular compartment, where water is more mobile. [60,61] On DW MR images, vasogenic edema may be hypointense to slightly hyperintense, because these images have both T2 and diffusion contributions. When vasogenic edema is hyperintense on DW MR images, it can mimic hyperacute or subacute infarction. On ADC images, cytotoxic edema due to ischemia is always hypointense for 1-2 weeks, and vasogenic edema is always hyperintense. Therefore, DW MR images should always be compared with ADC images. [60,61]

Correct differentiation of vasogenic from cytotoxic edema affects patient care. Misdiagnosis of vasogenic edema syndrome as acute ischemia could lead to unnecessary vasoactive agents. Furthermore, failure to correct relative hypertension could result in increased cerebral edema, hemorrhage, seizures, or death. Misinterpretation of acute ischemic infarction as vasogenic edema syndrome would discourage proper treatment with anticoagulants, evaluation for an embolic source, and liberal blood pressure control, which could increase the risk of recurrent brain infarction.

Hypoxic ischemic injury

Hypoxic ischemic injury (HII) refers to an imaging pattern of injury due to acquired global arterial hypoperfusion or global anoxia. Hypoxic ischemic encephalopathy (HIE) on the other hand refers to a clinical syndrome that often results from HII. Not all cases of HII lead to HIE. Many factors can increase the vulnerability and potential injury in HII.

The pattern of HII varies widely depending on the age of the patient. The different patterns of HII in term and preterms were explained by Osborn AG in Diagnostic imaging brain (2010) [62].

In preterm neonates the condition is referred to as white matter injury of prematurity (WMIP). It often occurs as focal white matter lesions adjacent to frontal horns or trigones of lateral ventricles. They are seen as hyperintense on T2W1 and iso to hypointense on T1W1. Deep gray nuclei, pons and cerebellar white matter can be involved. In late stages cyst formation and white matter volume loss can be seen. [62]

In term neonates, the pattern of involvement of the brain depends on the severity. In severe HII ventrolateral thalamus, corticospinal tract in posterior limb of internal capsule are most commonly involved. Cortex, thalamus, basal ganglia, hippocampi, dorsal brainstem and superior vermis can be involved in varying extent. On the other hand in partial HII, the ventrolateral thalamus and posterior limb of internalcapsule are spared. The predominant location is in cortex and subcortical white matter in the depth of sulci. In adults, HII usually results in infarcts in watershed areas of the brain. More severe insult may damage the basal ganglia, cortex, thalamus, hippocampi and cerebellum. [62]

DWI is the first imaging sequence to become positive, within hours of the event. Schaffer PW et al. in Diffusion weighted MR imaging of the brain (2000) [40] found in their study that diffusion restriction may be seen even when T1 and T2 images are normal. When lesions are identified on conventional images, lesion conspicuity is increased and lesion extent is seen to be larger on DW MR Images. In addition, lesions identified on the initial DW MR images are identified on follow-up conventional images and, therefore, help accurately predict the extent of infarction. [40]

Fu JH et al. in Early assessment of severe hypoxic-ischemic encephalopathy in neonates by diffusion-weighted magnetic resonance imaging techniques and its significance (2007) [63] found that though DWI is superior to the other imaging

modalities in detecting ischemia, diffusion restriction is not necessarily indicative of permanent damage. The abnormal image on DWI not last long. However, in chronic stage, the follow-up conventional MRI may compensate for this the inadequacy of DWI. [63]

Intracranial masses

Extra-axial masses

Conventional MR images cannot be used to reliably distinguish epidermoid tumors from arachnoid cysts; both lesions are very hypointense relative to brain parenchyma on T1-weighted MR images and very hyperintense on T2-weighted images. FU JH et al. (2007) [63] and Tsurdu J et al. in Diffusion-weighted MR imaging of the brain: value of differntiating between extra-axial cysts and epidermoid tumors. (2007) [64] found that epidermoid tumors are solid masses, however, which demonstrate ADCs similar to those of gray mater and lower than those of CSF. (63, 64) With the combination of T2 and diffusion effects, epidermoid tumors are markedly hyperintense compared with CSF and brain tissue on diffusion MR images. Conversely, arachnoid cysts are fluid filled, demonstrate very high ADCs and appear similar to CSF on DW MR images. Furthermore, on conventional MR images obtained after resection of an epidermoid tumor, the resection cavity and residual tumor may be similarly hypointense on T1-weighted images and hyperintense on T2-weighted images. On DW MR images, the hypointense CSF containing cavity can easily be differentiated from the residual hyperintense epidermoid tumor.

Intra-axial masses

DWI has been used to assess brain tumors and while it has had limited success as a definitive prognostic tool, its proponents suggest that in certain settings it can increase both the sensitivity and specificity of MR imaging. One example of a specific

arena in which DWI may be helpful is in distinguishing between brain abscesses and necrotic and cystic neoplasms on MRI. This differentiation is still a challenge on both clinical and radiological setting. Cruz CH et al. in Diffusion weighted MRI in brain tumor (2011) [10] showed that the abscesses have a high signal on DWI and a reduced ADC within the cavity as compared to necrotic tumors. [10]

Tein R et al. in MR imaging of high grade gliomas: value of difffusion-weighted echo-planar pulse sequences (1994) [60] and Els T et al. in Diffusion-weighted imaging of experimental brain tumors in rats (1995) [66] found that that tumor and edema have higher ADCs than does normal brain tissue and that central necrosis has a higher ADC than do tumor, edema, or normal brain tissue. ADC alone cannot be used to differentiate a nonenhancing tumor from adjacent edema. Brunberg et al. in In vivo MR determination of water diffusion coefficiets and diffusion aniotropy: correlation with structural alteration in gliomas of the cerebral hemispheres (1995) [70] and Schafer PW et al. (2000) [40] found that both enhancing and nonenhancing tumors can be distinguished from edema because edema has significantly higher indices of diffusion anisotropy when compared with adjacent tumor, presumably due to intact myelin within the edema. [40]

Tein R et al. in MR imaging of high grade gliomas: value of difffusion-weighted echo-planar pulse sequences (1994) [60] showed that in certain settings diffusion-weighted imaging can increase both the sensitivity and specificity of MR imaging in the evaluation of brain tumors by providing information about tumor cellularity, which may in turn improve prediction of tumor grade. The mechanism by which DWI may help in the tumor grading is based on the fact that free water molecule diffusivity is restricted by cellularity increase in high grade lesions. The reduction in extracellular space caused by tumor cellularity causes a relative reduction

in the apparent diffusion coefficient (ADC) values. Perhaps most helpfully, high grade tumors have in some studies been found to have low ADC values, suggesting a correlation between ADC values and tumor cellularity. [60]

Els T et al. in Diffusion-weighted imaging of experimental brain tumors in rats (1995) [66] however demonstrated in their studies that ADC values found in high and low grade gliomas have overlapped somewhat. It is well known that the brain tumors, specially the gliomas, are heterogeneous. Usually within a same neoplasm grade, mostly high grade, different histologic features of grades II – IV are presented. This limitation may also be explained by the fact that it is not only the tumor cellularity that is responsible for reducing the diffusibility. [66]

Lymphoma, a highly cellular tumor, has hyperintensity on DWI and reduced ADC values. While meningiomas also have a restricted diffusion, displaying low ADC values, they rarely present difficulty in diagnosis. Cruz CH et al. in Clinical experience with diffusion-weighted MR in patients with acute stroke. (2011) [10] found that DWI can be somewhat helpful in distinguishing medulloblastoma from other pediatric brain tumors, as it seems to display restricted diffusion presumably because of the densely packed tumor cells and high nuclear to cytoplasm ratio. The solid enhancing portion of cerebellar haemangioblastomas demonstrates high diffusibility, due to its rich vascular spaces. [10]

Infections

Pyogenic infections

Abscess cavities and empyemas are homogeneously hyperintense on DW MR images. Schafer P et al. in Echo planar diffusion weighted imaging in pyogenic infections (1997) [67] found that the relatively restricted diffusion most likely results from the high viscosity and cellularity of pus. [67]

Although intracranial abscesses and intracranial neoplasms may appear similar on images obtained with conventional MR sequences, Tein R et al. in MR imaging of high grade gliomas: value of diffusion-weighted echo-planar pulse sequences (1994) [60] and Kim Y et al. in Brain abscess and necrotic or cystic brain tumor: discrimination with signal intensity on diffusion-weighted MR imaging (1998) [68] demonstrated that the signal intensity of the abscess cavity is markedly higher and the ADC ratios are lower than those of necrotic tumors on DW MR images. [60, 68] Bacterial meningitis may be complicated by subdural effusions or subdural empyemas, which are difficult to differentiate on conventional MR images.

Empyemas are hyperintense on DW MR images and have restricted ADC, whereas sterile effusions are hypointense and have an ADC similar to that of CSF. Thus, DW MR images may be important when deciding whether to drain or conservatively mage extraxial collections associated with meningitis.

Cerebritis is the earliest manifestation of a pyogenic cerebral infection and is characterized by edema and perivascular exudates; it usually occurs 2-3 days following inoculation by the causative pathogen. In this phase, ill-defined infected tissue is hyperintense on FLAIR and T2-weighted MR images, whereas contrast enhancement is absent or minimal on T1-weighted images. In cases of cerebritis, Yilmaz et al. in Prediction of stroke outcome with echoplanar perfusion and diffusion-weighted MRI (2010) [69] showed that DWI of pyogenic infections reveals restricted diffusion and low ADC values, which have been attributed to hypercellularity, brain ischemia, or cytotoxic edema without purulent fluid. However, it is unusual for patients to present at this phase of cerebral infection, and imaging of early cerebritis has not been widely reported. [69]

Herpes encephalitis

Herpes encephalitis lesions are characterized by marked hyperintensity on DW MR images , with ADC ratios of these lesions to normal brain parenchyma ranging from 0.48 to 0.66. On follow-up conventional T1-weighted and T2-weighted MR images, these areas demonstrate encephalomalacic change. The restricted diffusion is explained by cytotoxic edema in tissue undergoing necrosis. Tein R et al. (1994) [60] and Brunberg J et al. (1995) [70] showed DW MR imaging may aid in distinguishing herpes lesions from infiltrative temporal lobe tumors because the ADCs of herpes lesions are low while the ADCs of various tumors are elevated or in the normal range. [60, 70]

Creutzfeldt-Jakob disease

Bahn M et al. in Brain magnetic resonance diffusion abnormalities in Creutzfeldt-Jakob disease (1997) [71] and Schaefer P et al. in Echo planar diffusion weighted imaging in Creutzfeldt-Jakob disease (1999) [72] showed that DW MR images in patients with Creutzfeldt-Jakob disease have demonstrated hyperintense lesions in the cortex and basal ganglia. [71, 72] Variable ADCs may be seen however, related to variable amounts of spongiform change, neuronal loss, and gliosis. Brown P et al. in Creutzfeldt-Jakob disease: clinical analysis of a consecutive series of 230 neuropathologically verified cases (1986) [73] and Johnson R et al. in Creutzfeldt-Jakob disease and related transmissible spongiform encephalopathies (1998) [74] found that while Creutzfeldt-Jakob disease is classically characterized by progressive dementia, myoclonic jerks, and periodic sharp-wave electroencephalographic activity, these features frequently are absent, and Creutzfeldt-Jakob disease cannot be clinically distinguished from other dementing illnesses. [73, 74] Furthermore Finenstaedt M et al. in MR imaging of Creutzfeldt-Jakob disease. (1996) [75] found

that conventional MR images may be normal in as many as 21% of patients. [75] Thus, DW MR imaging may be useful for help in the diagnosis of Creutzfeldt-Jakob disease and in the differentiation from Alzheimer disease.

Demyelination

Multiple Sclerosis

Christiansen P et al. in Increased water self-diffusion in chronic plaques and in apparently normal white matter in patients with multiple sclerosis (1993) [76] and Larsson H et al. in In vivo magnetic resonance diffusion measurement in brain of patients with multiple sclerosis (1992) [77] showed that acute plaques have significantly higher ADCs than do chronic plaques. [76, 77] The elevated diffusion may result from an increase in the size of the extracellular space due to edema and demyelination acutely and to axonal loss and gliosis chronically. In rare instances, acute plaques have restricted diffusion. This may result from increased inflammatory cellular infiltration with little extracellular edema. Of interest, is that normal appearing white matter has a mildly increased ADC. Allen IV et al. in A histological, histochemical and biochemical study of the macroscopically normal white matter in multiple sclerosis (1979) [79] found that this correlates with histologic results in which multiple sclerosis was shown to diffusely affect white matter. [79]

Osmotic myelinolysis

Osmotic myelinolysis is characterized by regions of demyelination throughout brain, most commonly in the pons. Extrapontine myelinolysis is most commonly seen in the basal ganglia, thalami and gray white matter junctions. Karaarslan E et al. in Diffusion-weighted magnetic resonance imaging in acute stroke (2008) [7] fund that characteristic MR findings of central pontine myelinolysis as symmetric T2-hyperintense lesions involving the basilar pons sparing the peripheral areas of pons

and descending corticospinal tracts. DWI shows areas of increased ADC similar to MS lesions. However, depending on the age of the lesions, not only degree of ADC elevation may vary, but also lesions with decreased ADC may be seen. [7]

Acute disseminated encephalomelitis

Acute disseminated encephalomyelitis lesions have ADCs higher than those of normal white matter, likely as a result of demyelination and increased extracellular water. DW MR imaging cannot help distinguish between multiple sclerosis and acute disseminated encephalomyelitis lesions because both usually have elevated diffusion. Because acute infarctions are characterized by restricted diffusion, however, DW MR imaging should be reliable for help in the differentiation between demyelinating lesions and stroke.

MATERIALS AND METHODS

The study was performed at the Department of Radio diagnosis, BLDEU's Shri B.M Patil medical College, Hospital and Research Centre, Vijayapur to describe the features of intracranial lesions on diffusion weighted imaging and to compare these features with ADC and T2 FLAIR images.

Source of data

The source of data for this study is patients referred to the Department of Radiodiagnosis, BLDEU's Shri B.M Patil medical College, Hospital and Research Centre, Vijayapur for MRI brain with diffusion weighted imaging. This consists of a study of 72 patients with intracranial lesions detected on imaging.

The MRI was done on the advice of the referring doctor and no patient was made to undergo MRI for the sole purpose of this study.

This dissertation evaluates the diffusion weighted imaging characteristics of intracranial lesions that were detected in these patients.

Study Period: October 2013 to July 2015

Study Design: Descriptive study

Inclusion criteria

The criteria for inclusion of the patients in the study included those patients who were clinically referred for diffusion weighted MRI of the brain and were detected to have any of the following;

1. Infarction and hypoxic ischemic injury
2. Infective conditions
3. Tumors – extra axial and intra axial
4. Demyelination
5. Metabolic or toxic insults to the brain
6. Degenerative disorders

Exclusion criteria

Patients who are detected to have intracranial bleed were excluded from the study.

Data Acquisition

Patients referred for diffusion weighted MRI of the brain, underwent the examination after contraindications for MRI were excluded and consent was taken.

All the MRI scans in this study were performed using 1.5 T MRI scanner (Philips Achieva).

MRI Protocol

MRI protocol consisted of the following

- A head coil was used
- Axial diffusion weighted images of the brain
- Axial T2W FLAIR images of the brain
- ADC images were reconstructed from the diffusion weighted images.

MRI procedure

All the patients are screened for the presence of :-

- Pacemakers
- Aneurysm clips
- Intra-ocular foreign bodies
- Metal devices or prostheses
- Cochlear implants
- Spinal implants and stimulators
- Possibility of early pregnancy
- Jewellery, credit cards, money, watches, etc.

The patient lies supine on the examination couch with head within the head coil. The head is adjusted so that the inter-pupillary line is parallel to the couch and the head is straight. The patient is positioned so that the longitudinal alignment light lies

in the midline, and the horizontal alignment light passes through the nasion. Straps and foam pads are used for immobilization.

Slice thickeness

Medium slices/gaps are prescribed from below the foramen magnum to the superior surface of the brain. Slices are angled in such a way that they are parallel to the anterior–posterior commissure axis, so as to allow precise localization of lesions from reference anatomy atlases

A b-value of 800–1000 s/mm2 is selected (the higher the b-value, the more diffusion weighting). Isotropic diffusion is acquired (i.e. diffusion gradients applied in all three axes)

The DWI sequence is acquired using a T2-weighted EPI sequence. The b-value controls the amplitude, duration and/or timing of these diffusion gradients and thus determines the amount of diffusion weighting in a diffusion sequence. Increasing the b-value increases the sensitivity to the motion (diffusion) of extracellular water in tissue and thus increases the diffusion weighting. The signal in areas of normal diffusion is reduced due to the dephasing of the water protons in the presence of these diffusion gradients. The more restricted the diffusion, the less dephasing of the water protons and higher signal will be seen on the diffusion image. Both the b = 0 image (i.e. the T2-weighted EPI image) and the diffusion image with the b value chosen by the operator are displayed.

The ADC image may be produced automatically from the diffusion weighted images.[83]

RESULTS

The present study was carried out to describe imaging characteristics of intracranial lesions on DWI and to compare them with ADC and T2 FLAIR images. Findings in the patients studied were tabulated using Microsoft Excel and has been given as Annexure. All statistical analyses were conducted using the SPSS statistical package.

Data analysis

72 cases of intracranial lesions were included in the study. The observations of these 72 patients were compiled and analyzed.

Age wise distribution of intracranial lesions

The age of the patients with intra cranial lesions studied ranged from 2 months to 85 years with a mean of 43.97 ± 2.04.

The patients involved in the study were divided into 9 age groups viz. 1-10 years, 11-20 years, 21-30 years, 31-40 years, 51-60 years, 61-70 years, 71 – 80 years and 81-90 years. There were eight patients (11.11%) in 1-10 year group, two (2.77%) in 11-20 year age group, two (2.77%) in 21-30 year age group, four (5.55%) in 31-40 year age group, eleven (15.27%) in 41-50 year age group, eighteen (25%) in 51-60 year age group, nineteen (26.38%) in 61-70 year age group, six (8.33%) in 71-80 year age group and two (2.77) in 81 – 90 years age group as given in table below.

Chart 1 Age distribution of intracranial lesions

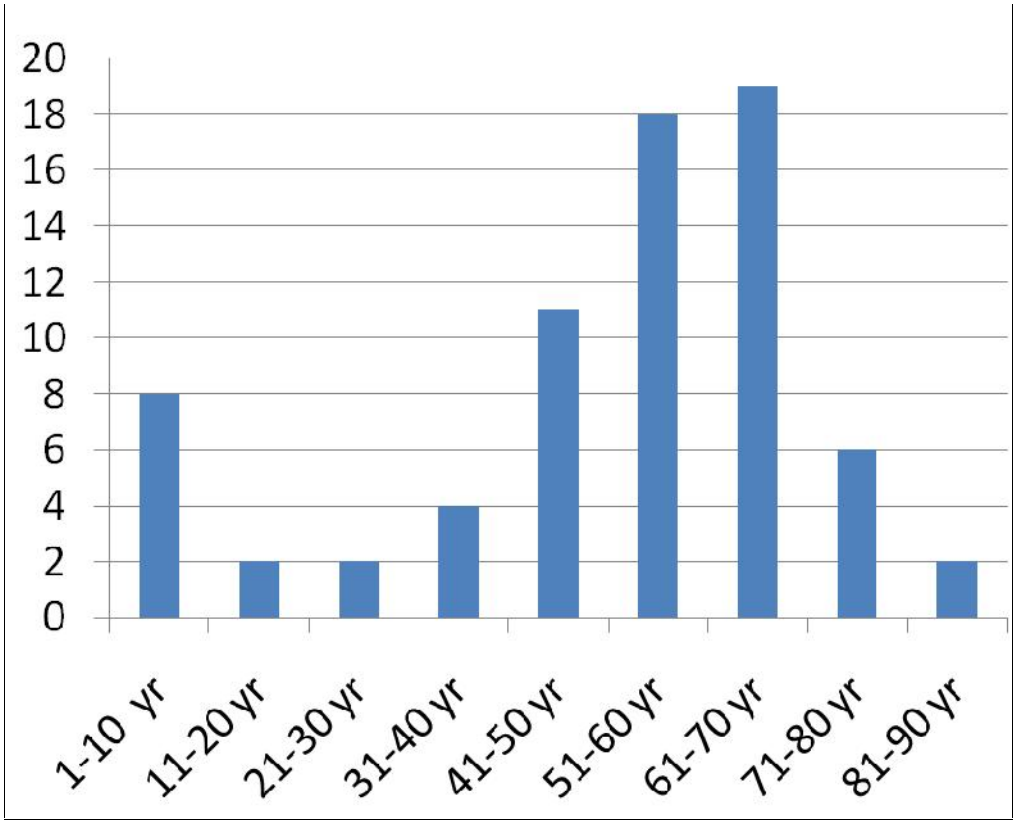

Sex wise distribution of intracranial lesions

Of the 72 patents studied 44(61.11%) were and 28(38.88%) were females.

Chart 2 Sex Wise Distribution Of Intracranial Lesions

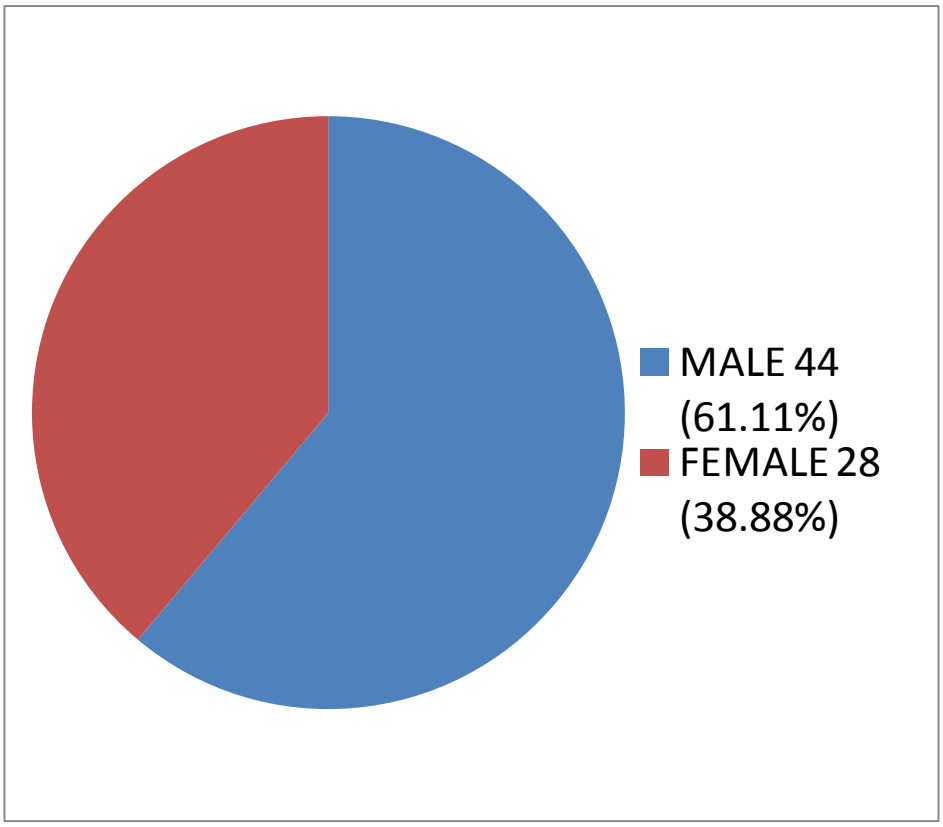

7.1.3 Spectrum of intracranial lesions

Of the total cases included in this study, infarcts were the majority which constituted 32 cases (44.44%), 3 cases of hypoxic ischemic encephalopathy (4.16%) were also included. The other cases were 24 cases of tumors (33.33%) of which 14 (58.33%) were intra axial and 10 (41.66%) were extra axial tumors, 9 infective conditions (12.5%), 2 cases of demyelination (2.77%) and 2 other miscellaneous conditions (2.77%). These included 1 case of periventricular leucomalacia, and 1 case of posterior reversible encephalopathy syndrome.

Chart 3 Types of intracranial lesions

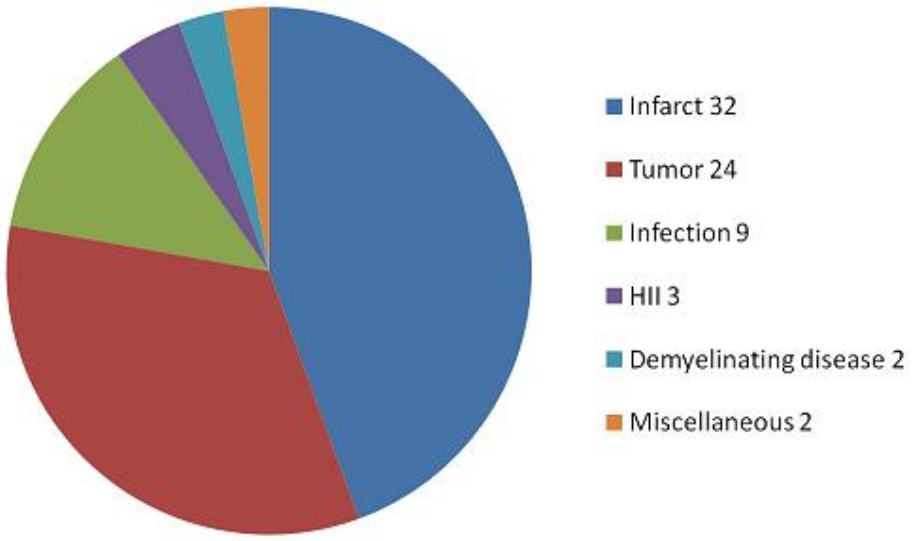

Imaging characteristics of intracranial lesions

MR appearance

Of the 72 patients included in this study, 51 cases (70.8%) showed hyperintensity on DWI of which true restriction (hyperintense on DWI and hypointense on ADC) was noted in 52 patients (45.2%). This constituted 63.4% of the cases showing diffusion restriction. T2 shine through was noted in 30 patients (26%). This constituted 36.6% of the cases showing diffusion restriction.

52 cases (45.2%) showed hypointensity on ADC images. All of these were hyperintense on DW images. 13 patients (11.3%) showed T2 washout (hyperintense on T2WI and isointense on DWI). 5 patients (0.43%) showed no signal change on DWI or ADC images. 51 patients (44.3%) had lesions that showed increased diffusivity (hyperintense signal on ADC image). Of these 15 (13%) were hypointense on DWI. This constituted 29.4% of the cases showing increased diffusivity. 13 of these showed T2 washout, and 23 showed T2 shine through.

Infarcts

Infarcts constituted 32 cases (44.44%) of the total cases in this study. Of this 19 (59.3%) were acute infarcts, 10 (31.25%) were chronic infarcts and 3 (9.3%) were subacute infarcts. There were 24 (75%) males and 8 females (25%) among these cases.

In 20 cases (62.5%) the infarcts were in MCA territory, in 4 cases (12.5%) they were in ACA territory, in 6 cases (18.75%) the infarcts were in PCA territory and in 2 cases (6.25%) they were in basilar artery and vertebral artery territory.

Chart 4 Distribution of infarcts

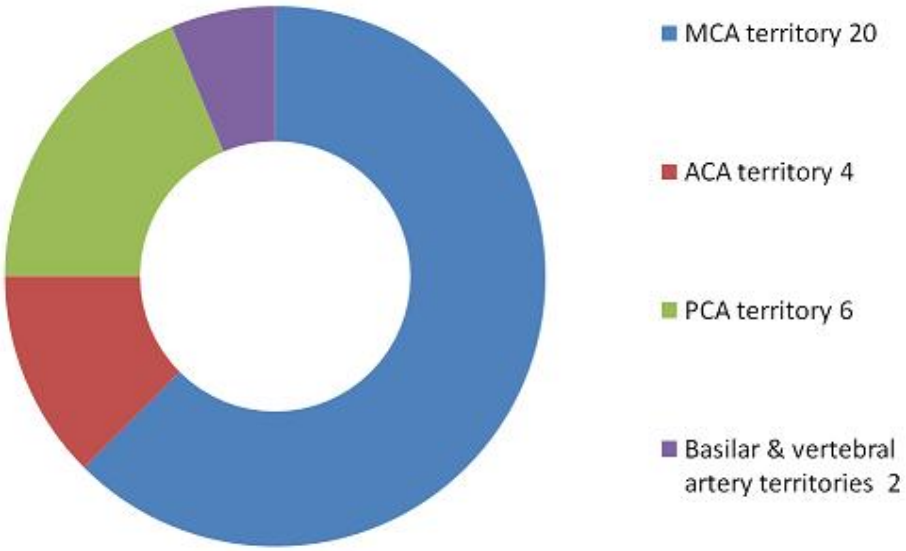

All 19 cases (100%) of acute infarcts showed true diffusion restriction with hyperintensity on DWI and hypointensity on ADC images. Of these, 16 cases (84.21%) showed hyperintensity on T2W images. The remaining 3 cases (15.78%) showed no signal change on T2W images.

Of the 10 cases of chronic infarcts, ADC signal was increased in all, suggesting increased water diffusivity. In 5 cases (50%), there was hypointensity on DWI and T2 FLAIR images with hyperintensity on ADC images indicating

encephalomalacic changes. T2 shine through was noted in 5 cases (50%). None of the cases showed T2 washout.

Out of 3 cases of subacute infarcts, and 2 (66.66%) showed T2 shine through.

Hypoxic ischemic injury

Three cases of hypoxic ischemic injury were included in this study. Two cases were preterm neonates and one was a term neonate.

All three cases showed true diffusion restriction. 2 (66.66%) showed hyperintensity on T2 FLAIR images, and 1 (33.33%) did not show any change on T2 FLAIR images.

The extent of abnormality was noted to be more on DW and ADC images than on T2 FLAIR images.

Infections

The study included 9 infective conditions of which 4 (44.44%) were tubercular s, 2 (22.22%) were NCC granulomas, 1(11.11%) was abscesses, 1 (11.11%) was extradural empyemas and 1 case (11.11%) was HSV encephalitis.

True restriction of diffusion was noted in 5 (55.55%) cases. This included 3 tubercular granulomas, 1 abscess and 1 extradural empyemas. Thus 75% of tubercular granulomas, 100% of abscesses and 100% of extradural empyemas showed true diffusion restriction.

T2 washout was seen in all 2 cases (100%) of NCC granulomas.

T2 shine through was seen in 1 case of tubercular granuloma and one case of HSV encephalitis.

Tumors

There were total of 24 cases of tumors.

Intra axial tumors

There were 14 (58.33%) cases of intra axial tumors in this study. The patients consisted of 10 (71.42%) males and 4 females (28.57%). This included 2 cases of anaplastic astrocytoma, 4 cases of glioblastoma multiforme, 3 cases of low grade gliomas, 2 cases of medulloblastomas, 1 case of pilocytic astrocytoma, 1 case of hemangioblastoma and one case of lymphomas.

5 cases (35.71%) showed true diffusion restriction. Of these were 2 were GBM, 2 were medulloblastomas, and 1 was lymphoma. Thus 50% of GBM, 100% of medulloblastomas, and 100% of lymphomas showed true restriction of diffusion.

Chart 5: Intra axial tumors

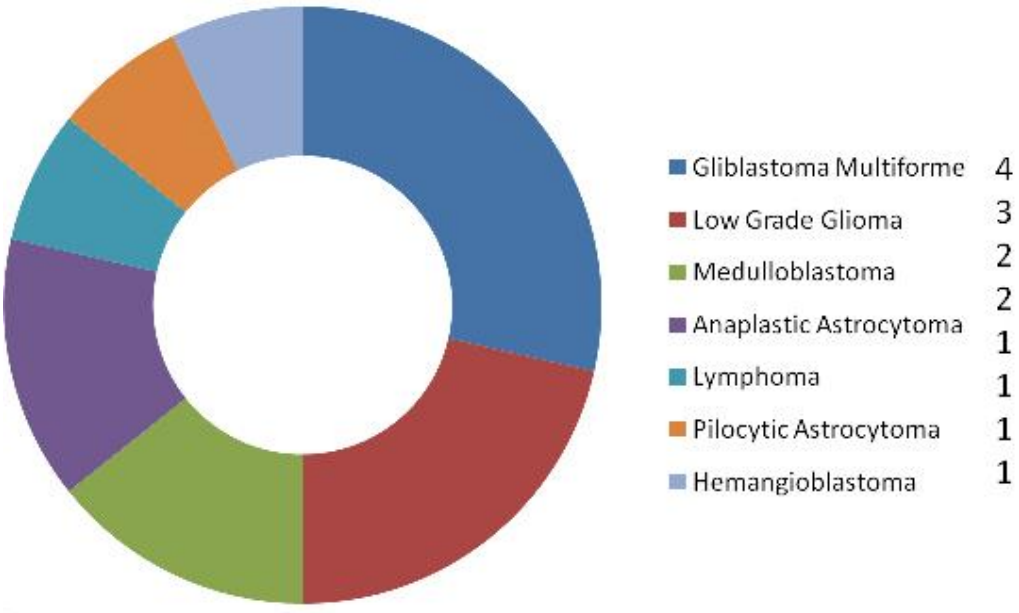

T2 shine through was noted in 6 cases (42.85%).

T2 washout was seen in one case of hemangioblastoma and 2 cases (66.66%) of low grade gliomas.

Extra axial tumors

10 (41.66%) cases of extra axial tumors were included in this study Of these 7 were males and 3 were. There were 5 cases of meningioma, 3 cases of arachnoid cyst, 1 case of epidermoid cyst and 1 case of schwannoma. True restricted diffusion was noted in 4 cases (25%). This included the single case of epidermoid cyst and 3 cases (60%) of meningiomas. In one case of meningioma, T2 shine through was noted. In 1 (20%) cases of meningiomas, T2 FLAIR showed iso to hypointense signal probably due to high cellularity and presence of calcification. 1 case (100%) of schwannoma showed T2 washout.

Chart 6 Extra axial tumors

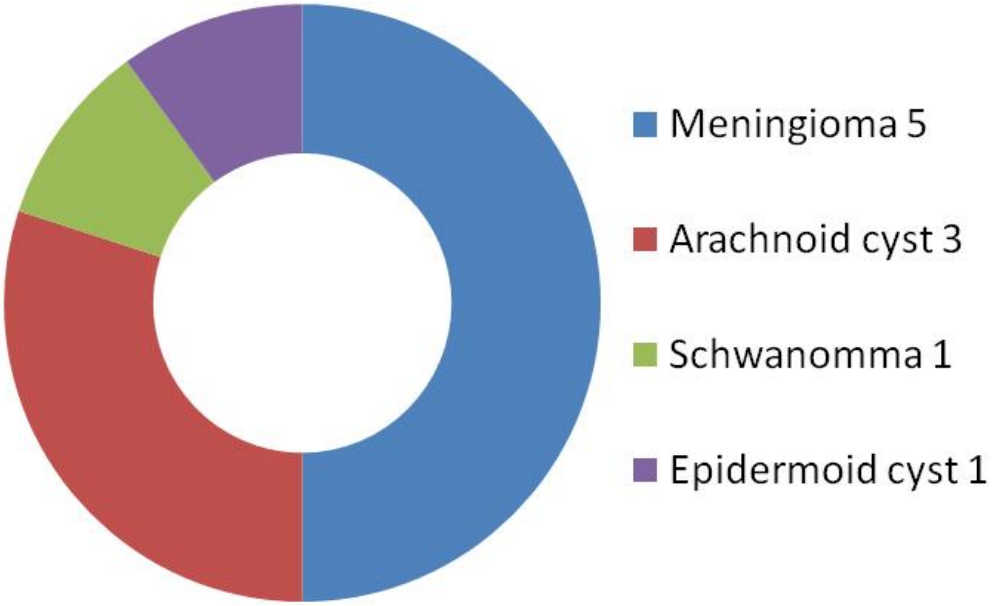

Demyelination

Two cases of demyelination were noted in this study, this included one case each of multiple sclerosis and ADEM Both the lesions showed hyperintensity on T2 FLAIR images. True restriction of diffusion was not noted in any of the cases. T2 washout was seen in the case of multiple sclerosis. No change was noted on DWI or ADC images in the case of ADEM.

Miscellaneous other lesions

This group consisted of 1 case of periventricular leucomalacia and 1 case of posterior reversible encephalopathy syndrome (PRES).

All the lesions showed hyperintensity on T2 FLAIR images. True restriction of diffusion was not noted in any of the cases. T2 washout was seen in the case of PRES.

Representative cases

Some of the representative cases have been reported in detail, in the following section along with their respective images.

CASE No. 1

Age: 55 years

Sex: Male

Clinical data: Well defined DWI and T2 FLAIR hyperintense area in right corona radiate. The corresponding area is hypointense on ADC images. Multiple other scattered white matter T2 FLAIR hyperintense foci are noted which do not show diffusion hyperintensity.

Diagnosis: Acute infarct in right corona raidata.

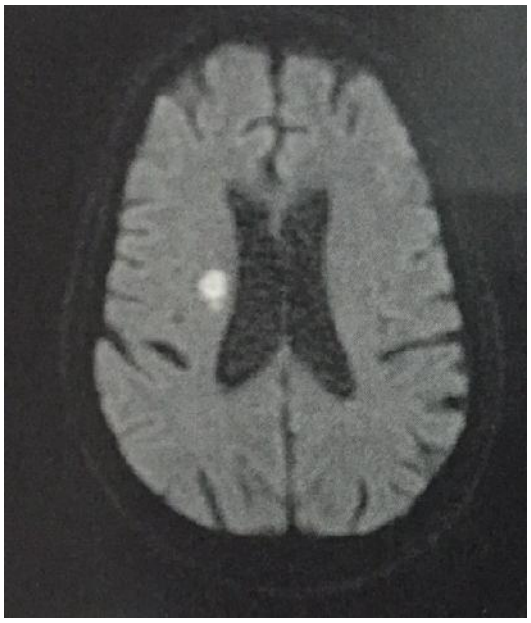

Axial DW image

Axial T2FLAIR image

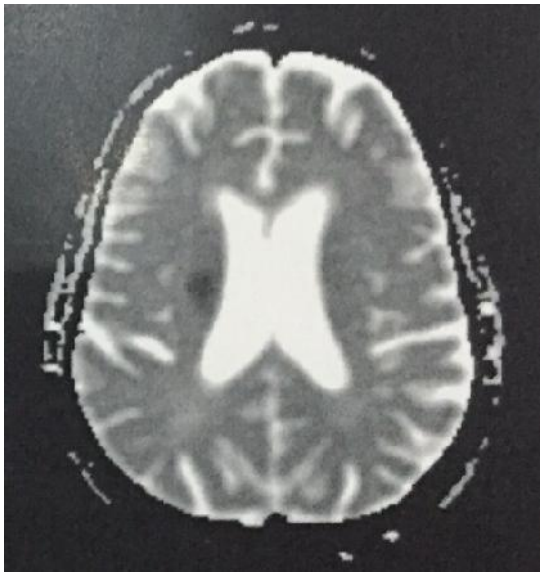

Axial ADC Image

CASE NO. 2

Age: 61 Years

Sex: Male

Clinical data: Headache and right sided weakness for one month.

Findings: T2 FLAIR and DWI images show hypointense cystic areas in left MCA and PCA territory. Corresponding areas are hyperintense on ADC images. There is volume loss with ex-vacuo dilatation of the ipsilateral lateral ventricle.

Diagnosis: Chronic infarct in left MCA and PCA territory with cystic encephalomalacia.

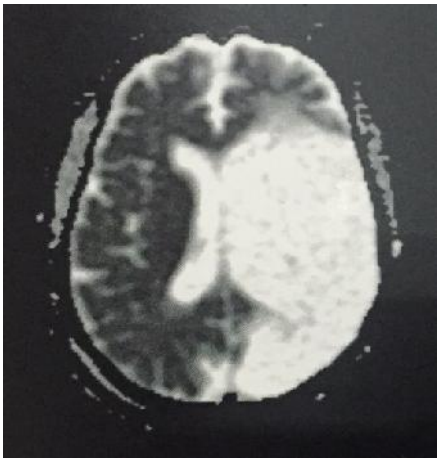

Axial ADC image

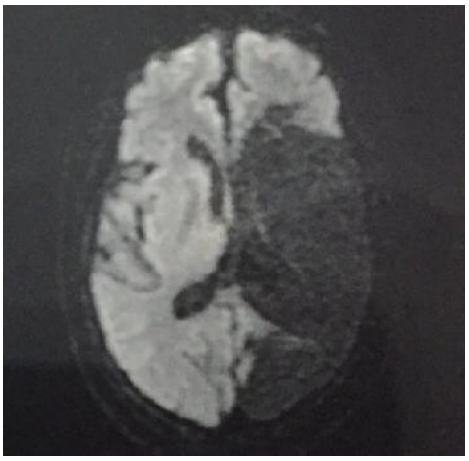

Axial DW image

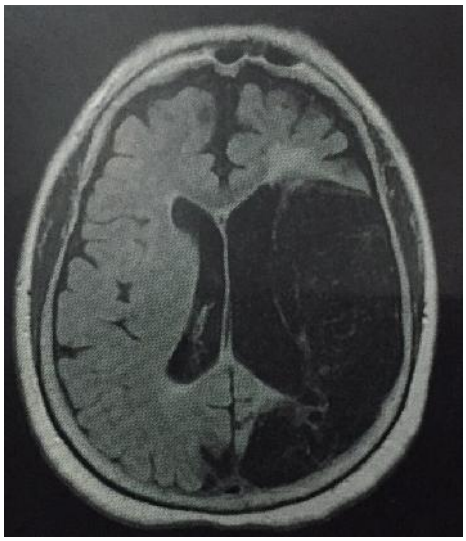

Axial T2FLAIR image

CASE NO. 3

Age: 11 Years

Sex: Male

Clinical data: Headache, projectile vomiting, unsteadiness.

Findings: Posterior fossa mass lesion arising from the roof of fourth ventricle and vermis. The mass is hyperintense on DWI, isointense on T2 FLAIR image and hypointense on ADC image. There is compression of fourth ventricle with resultant hydrocephalus and periventricular ooze.

Diagnosis: Medulloblastoma.

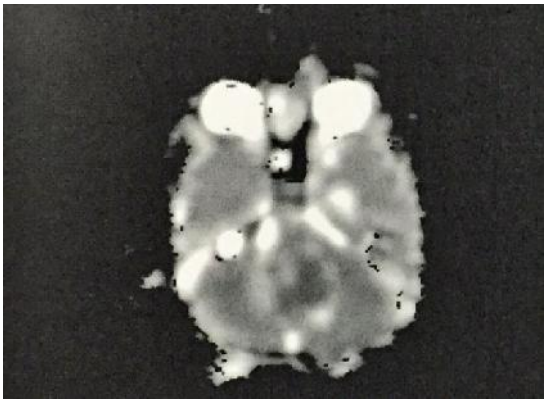

Fig Axial ADC image

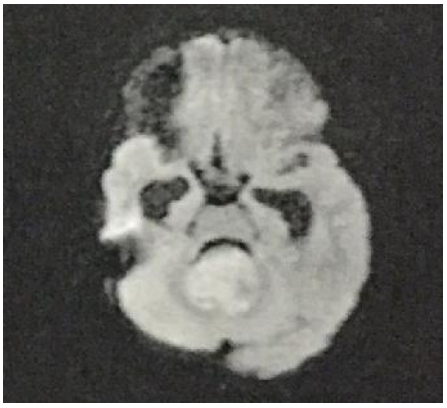

Axial DW image

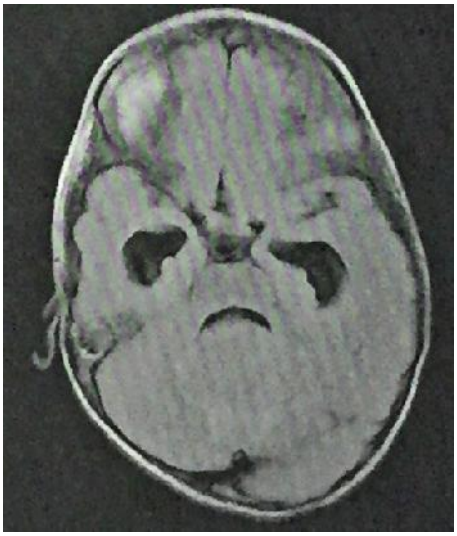

Fig T2 FLAIR image

CASE NO. 4

Age: 10 days

Sex: Female

Clinical data: Term neonate with history of birth asphyxia, poor cry at birth, low GCS and seizure.

Findings: Diffusion hyperintensity and ADC hypointensity noted involving both parietal and occipital lobes more on right side, and in both ventrolateral thalami, posterior limb of internal capsule and in splenium of corpus callosum. There is faint T2 FLAIR hyperintensity in both parieto-occipital lobes.

Diagnosis: Profound term hypoxic ischemic encephalopathy.

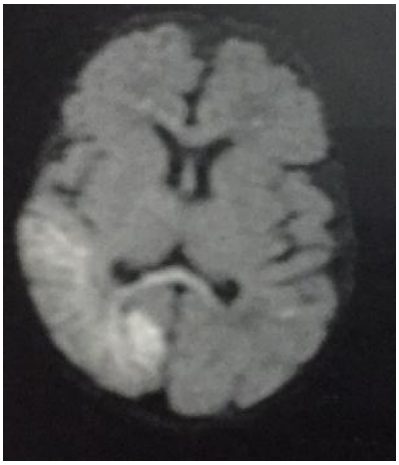

Axial DW image

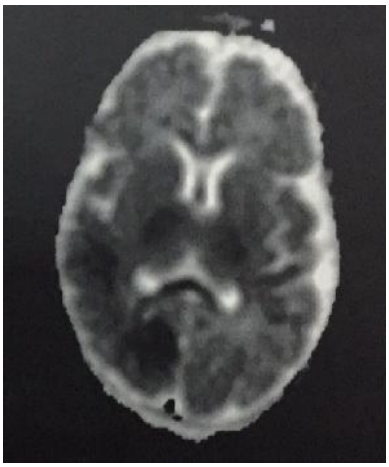

Axial ADC image

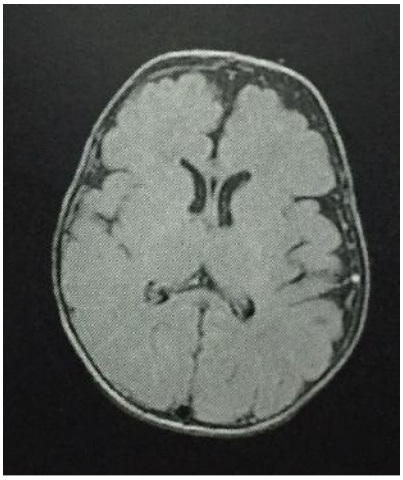

Axial T2FLAIR image

CASE NO. 5

Age: 24 Years

Sex: Male

Clinical data: Headache.

Findings: Well defined T2 FLAIR hypointense extra-axial mass lesion noted in left anterior temporal region. It is hypointense on DW image and hyperintense on ADC. It is mildly displacing the adjacent temporal lobe. However there is not edema in the adjacent brain parenchyma.

Diagnosis: Arachnoid cyst.

Axial DW image

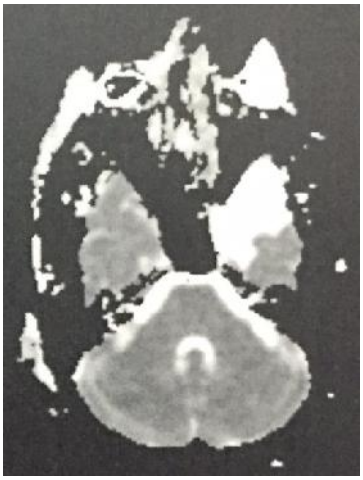

Axial ADC image

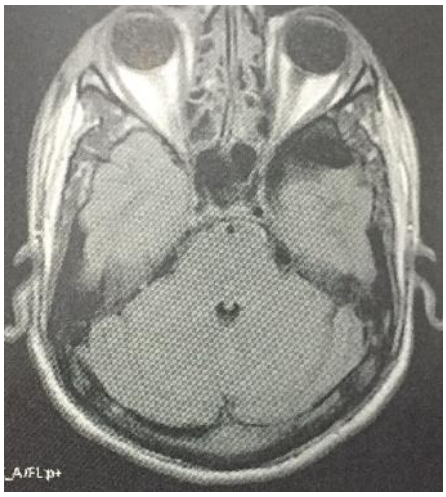

Axial T2FLAIR image

CASE NO. 6

Age: 27 Years

Sex: Male

Clinical data: Bi-frontal headache for 1 month worsened over past few days.

Findings: Left frontal extra axial extradural collection noted. It is hyperintense on DWI, hypointense on ADC and isointense on T2 FLAIR images. Mucosal thickening noted in both frontal sinuses.

Diagnosis: Left frontal extra dural empyema.

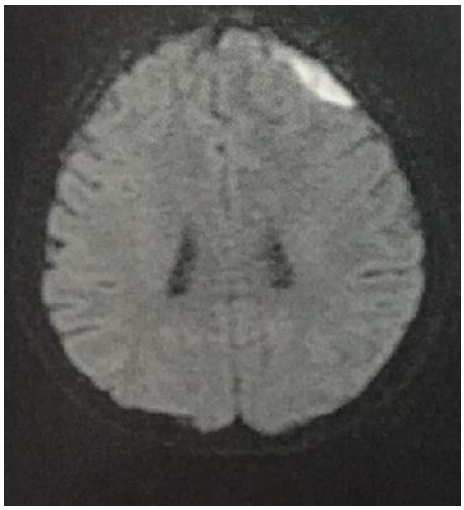

Axial DW image

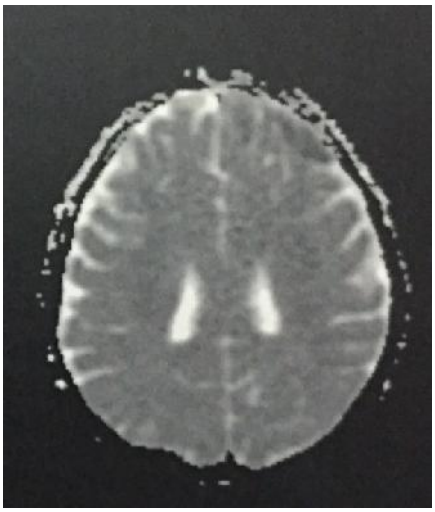

Axial ADC image

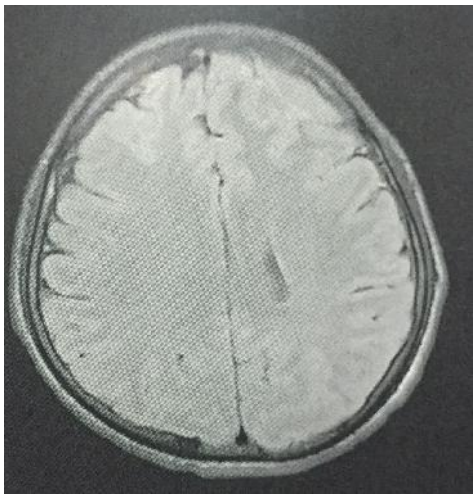

Axial T2FLAIR image

CASE NO. 7

Age: 64 Years

Sex: Male

Clinical data: Headache, vomiting, seizure, episodes of altered sensorium.

Findings: Large left sided intra axial mass noted involving left frontal, parietal and temporal lobes. Areas of hemorrhage noted. Patchy areas of DWI hyperintensity and ADC hypointensity noted. There is adjacent edema and mass effect with midline shift of 8 mm to left.

Diagnosis: Glioblastoma multiforme.

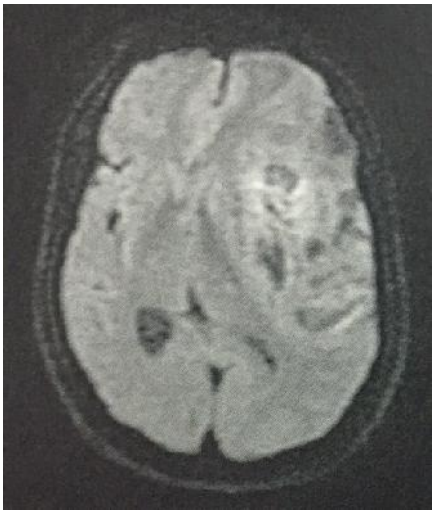

Axial DW image

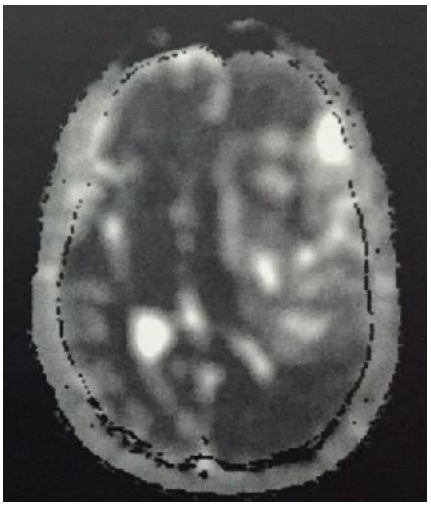

Axial ADC image

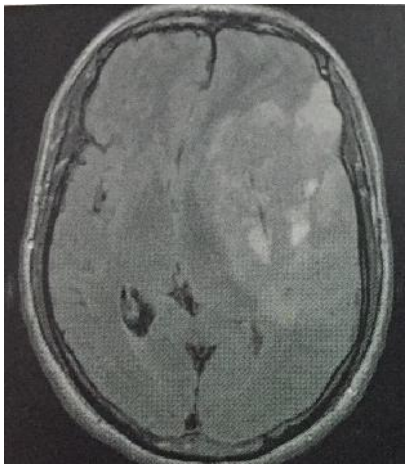

Axial T2FLAIR image

CASE NO. 8

Age: 15 Years

Sex: Male

Clinical data: Headache, vomiting, high grade fever, altered sensorium.

Findings: Well defined round lesion with a T2 hypointense and T1 isointense rim noted in right frontal region. The centre of the lesion is hyperintense on DWI and hypointense on ADC and T2 FLAIR images. There is moderate adjacent edema and mass effect with midline shift of 7 mm to left.

Diagnosis: Cerebral abscess.

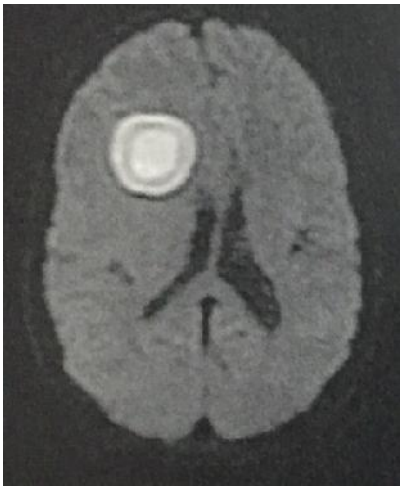

Axial DW image

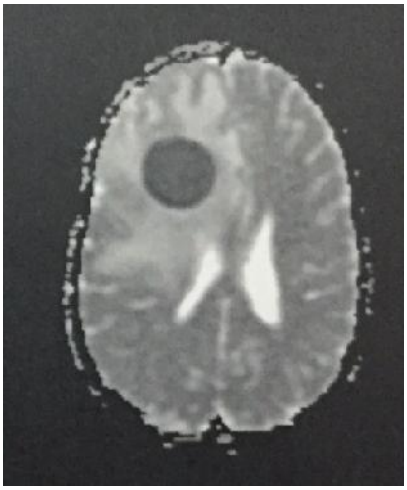

Axial ADC image

Axial T2FLAIR image

CASE NO.9

Age: 42 Years

Sex: Female

Clinical data: Headache, vomiting.

Findings: Well defined extra axial mass lesion is noted arising from the anterior falx. It is isointense on T1W image and shows patchy areas of hyperintensity on DWI and hypointensity on ADC images. There is mass effect on the adjacent frontal lobe with edema in the brain parenchyma.

Diagnosis: Meningioma.

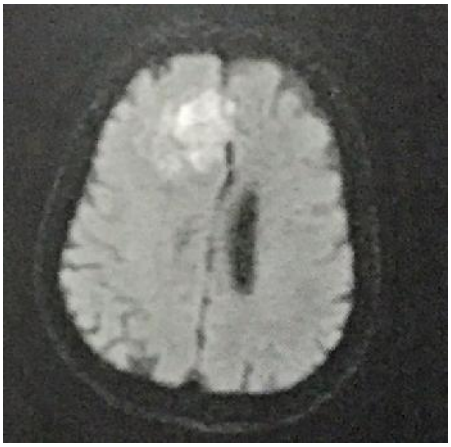

Axial DW image

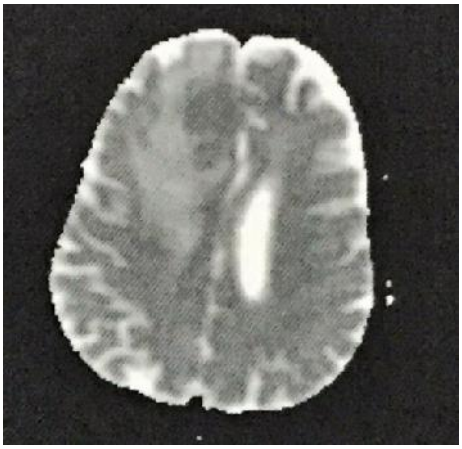

Axial ADC image

Axial T2 FLAIR image

CASE NO. 10

Age: 63 Years

Sex: Male

Clinical data: HRV positive patient, headache, altered sensorium.

Findings: Heterogeneous intra axial mass lesion is noted in the right parietal lobe. There is moderate mass effect and adjacent edema. It is mildly hypointense on T2 FLAIR images, hyperintense on DWI and hypointense on ADC images. There is involvement of the splenium of corpus callosum.

Diagnosis: Lymphoma.

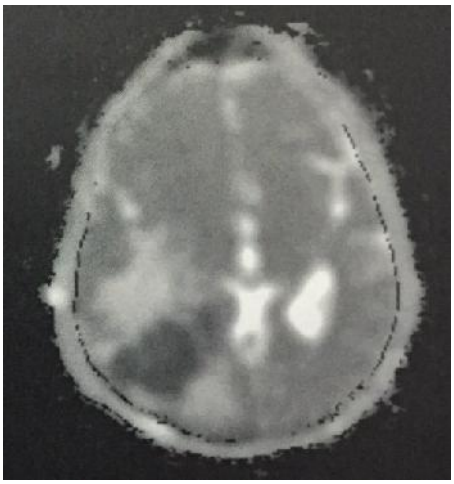

Axial ADC image

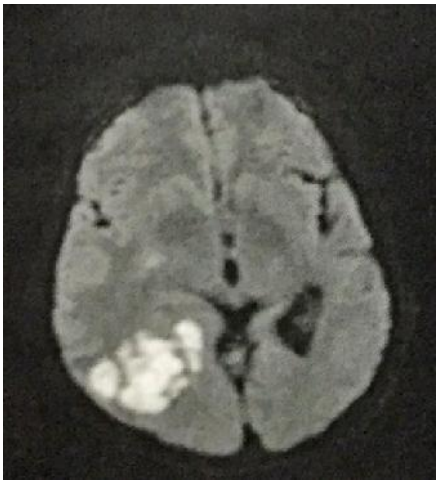

Axial DW image

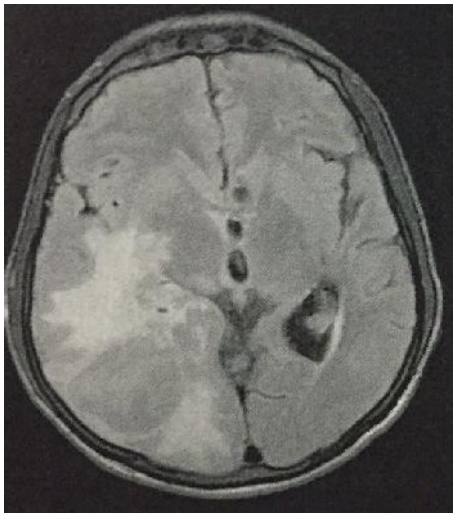

Axial T2FLAIR image

DISCUSSION

Diffusion weighted MRI provides image contrast that is different from that provided by conventional MRI sequences. It provides a technique for mapping proton contrast that reflects the microvascular environment. This imaging technique is sensitive to early ischemic insult. DWI is performed with a pulse sequence capable of measuring water translation over short distances. This water diffusion is much slower in certain pathological conditions as compared with normal brain. (80)

In this study 72 patients with intracranial lesions detected on DW MRI of the brain were included. It was found that DW MRI provides adjunctive information for intracranial lesions including stroke, neoplasms, infections, hypoxic ischemic encephalopathy and extra axial lesions in conjunction with conventional MRI.

Infarcts and HII

Infarcts

The sensitivity and specificity of DWI in the detection of acute ischemia is 100%. The difference in sensitivity of DWI and conventional MRI sequences is more in the initial time period and decreases as time progresses. Results of this study are correlated with a study done by **Gonzalez et al**, **in Diffusion-weighted MR imaging: diagnostic accuracy in patients imaged within 6 hours of stroke symptom onset.** [(52)] in which they obtained a sensitivity and specificity of 100% for patients diagnosed as having and not having acute stroke and thus concluded that DWI is superior to conventional MRI in the diagnosis and characterization of acute infarct.

K.J. van Everdingen et al. **in Diffusion-Weighted Magnetic Resonance Imaging in Acute Stroke** were able to diagnose 98% of acute infarcts on DWI and while on T2 FLAIR they were able to diagnose 90% of acute infarcts.[(84)]

In this study restricted diffusion was noted in 100% of acute infarcts. In 3 (15.78%) of acute infarcts, no change was noted on T2W1. Thus DWI was noted to be superior to T2W1 in detection of acute infarcts.

In **subacute infarcts** and chronic infarcts, abnormal signal was noted on T2 FLAIR and on DWI in all patients. Thus there was a decrease in difference of their sensitivity for later stages of infarcts.

Rima K et al, **in Role of diffusion weighted MR imaging in early diagnosis of cerebral infarction** [80] showed that restricted diffusion is present in all patients on DW MR studies obtained within 24 hours of the onset of symptoms, and in 94% of patients scanned after 2 weeks after ictus. In this study subacute infarcts were defined as patients in whom imaging was performed between 2 and 14 days after symptom onset. [62] True diffusion restriction was noted in 50% of patients with subacute infarcts. The other 50% showed T2 shine through. Thus all the patients with subacute infarct showed T2 FLAIR abnormality

Similarly, **Augustin M et al. in Diffusion-weighted imaging of patients with subacute cerebral ischemia: comparison with conventional and contrast-enhanced MR imaging,** [85] found that subacute infarct was detected by DWI in 93% of cases and by T2 FLAIR in 79% of the cases. This again proves that there is a decrease in difference of sensitivity in case of subacute infarct.

In this study 20 (62.5%) of infarcts were noted to be in MCA territory, 6 (18.75%) in PCA territory, 4 (12.5%) in ACA territory and 2 (6.25%) in vertebral artery and basilar artery territory. This is comparable to a study done by **Van Der Zwan et al, Variability of the major cerebral arteries** [81] which showed that MCA territory is the most common site for infarcts.

In **chronic infarcts** the signal on DWI and ADC images is variable and depends on a combination of T2 FLAIR signal and increased ADC values. The T2 FLAIR signal is also affected by the onset of cystic encephalomalacia as seen by **Schafer PW, et al, in Diffusion weighted MR imaging of the brain.** [40]

In this study T2 shine through was noted in 55.5% of chronic infarcts and cystic encephalomalacia was noted in 44.4%.

Hypoxic ischemic injury

Diffusion-weighted imaging has proved to be more sensitive than conventional MR imaging sequences for early detection of hypoxic ischemic brain injury. **Fu JH et al**, (63) compared conventional MRI sequences to DWI in the evaluation of HII and found that DWI showed abnormal high signal intensity in the brain in patients in whom the conventional MR sequences were initially normal. He concluded that HII lesions not seen on routine MR images are identified on DW MR images. When lesions are identified on conventional images, lesion conspicuity is increased and lesion extent is seen to be larger on DW MR images.

Alexander M. McKinneya et al. in Diffusion-Weighted Imaging in the Setting of Diffuse Cortical Laminar Necrosis and Hypoxic-Ischemic Encephalopathy **found DWI in all 6 patients subjected to DWI and ADC imaging, while T2 FLAIR was able to pick up abnormality in only 1 patient.[86]**

Choi HY et al. in Diffusion-weighted MR Imaging of Hypoxic-Ischemic Encephalopathy, studied features of T2 FLAIR and DWI in 6 patients of HII,[88] they found that for basal ganglia lesions DWI produced better lesion conspicuity in 4 cases, for cortical and subcortical lesions DWI produced better lesion conspicuity in 3 cases, for deep cerebral white matter lesion conspicuity with DWI was better in only one case.

All cases of neonatal HII included in this study showed true diffusion restriction. In 1 (33.33%) of cases there was no abnormality on T2 FLAIR images. The extent of abnormal signal was much more in the remaining cases on DWI, than that showed by T2W images.

Infections

Several studies have showed that DWI can differentiate necrotic tumors from abscesses as both can show rim like enhancement on post contrast images.

Chang SC et al. in Diffusion weighted MRI features of brain abscess and cystic or necrotic tumors – comparison with conventional MRI have showed that abscess cavity shows high signal intensity on DWI and a low signal on ADC image. This is not seen in the necrotic component of brain tumors. They concluded that DWI may enable one to distinguish brain tumors from necrotic tumors. Also it helps in the evaluation of partially treated abscesses and to look for their recurrence.

Kim et al. in Brain abscess and necrotic or cystic brain tumor: discrimination with signal intensity on diffusion-weighted MR imaging [(69)], found hyperintense signals on DWI in all the four cases of abscess and they found DWI hypointensity in all the four cases of cystic or necrotic brain tumors examined.

In this study 100% of cases of abscess showed true diffusion restriction. The cystic or necrotic component of none of the tumors included in this study showed restricted diffusion.

In all 4 (100%) of the tubercular granulomas observed in this study, diffusion restriction was noted, probably denoting presence of necrosis. One (25%) of tubercular granulomas and 100% of NCC granulomas could not be detected on DWI alone and needed ADC and T2W images for lesion detection probably due to the poor spatial resolution of diffusion weighted imaging.

The only case of extradural empyema noted in this study showed true diffusion restriction. The thick nature of this collection causes reduced water diffusivity similar to abscesses.

Tumors

Intra axial tumors

MR imaging is the most sensitive method of detecting tumors of the brain. It is however not specific enough to determine the histological nature of most tumors. DWI can differentiate between tumor and infection and can provide information about the cellularity of tumors thereby helping in characterization and grading of tumors as seen in the study **Mortani T, et al**. **Diffusion weighted MR imaging of the brain** [82].

Cruz CH et al, in Diffusion weighted MRI in brain tumor [10] showed that highly cellular tumors such as high grade gliomas and lymphomas can have low ADC values and show restricted diffusion. It was also shown that medulloblastomas may be differentiated from other pediatric brain tumors by presence of diffusion restriction. The solid portion of hemangioblastomas has high ADC values due to their rich vascular spaces.

In this study 2 (50%) of the glioblastoma multiforme, 2 (100%) of the medulloblastoma and 1 (100%) lymphoma showed true diffusion restriction, suggesting a high cellularity.

In accordance with (10) single case of hemangioblastoma seen in this case showed high signal on ADC in its solid component suggesting high water diffusivity.

Extra axial Tumors

Diffusion weighted MR plays a key role in differentiating arachnoid from epidermoid cysts. **Schaefer et al, in Diffusion weighted MR imaging of the brain** [40] showed that conventional MR cannot be reliably used to differentiate these two lesions as both have CSF like signal intensity on conventional MR sequences. However on DWI epidermoid cyst shows restricted diffusion while arachnoid cyst shows CSF like intensity

This was also demonstrated in a study by **Cruz et al. in Diffusion weighted MRI in brain tumor** [10], in which epidermoid cysts had ADC values similar to brain parenchyma while arachnoid cysts had ADC values similar to CSF.

In this study all 3 cases of arachnoid cysts had signal similar to CSF on DWI and ADC images. The single case of epidermoid cyst noted in this study had restricted diffusion.

Tadeusz et al in Differential diagnosis of bright lesions on diffusion weighted MR images. [3] And **Cruz et al in Diffusion weighted MRI in brain tumor** [10] concluded that most meningiomas are isointense on DWI and only few may show restricted diffusion depending on their cellularity. In their study 23% of meningiomas showed restricted diffusion. However, in this study 3 (60%) of the meningiomas showed true restricted diffusion.

Demyelination

Most demyelination plaques which may or may not be part of multiple sclerosis have been shown to have increased ADC values. It is very rare for a plaque to show restricted diffusion. Studies done by **Christiansen P et al**, i**n increased water self-diffusion in chronic plaques and in apparently normal white matter in patients with multiple sclerosis [76] and Larsson H et al, in In vivo magnetic**

resonance diffusion measurement in brain of patients with multiple sclerosis [77] have shown that most foci of demyelination do not show restricted diffusion.

Similar to the above stated two studies the two cases of demyelination seen in this study did not show restricted diffusion and had increased signal on T2 FLAIR images.

Others

Schwartz et al, in Diffusion-weighted MR imaging in hypertensive encephalopathy: clues to pathogenesis [61] showed that the PRES showed restricted diffusion. The results of this study are similar. [61]

No signal change was noted in periventricular leukomalacia seen in this study.

CONCLUSION

The objectives of this study were to describe the features of intracranial lesions on DWI and to compare these features with ADC and T2 FLAIR images. DW MRI study was undertaken in 72 patients admitted to the BLDEU's Shri B.M Patil Medical College, Hospital and research Centre, Vijayapur with suspected intracranial lesions. All the MRI scans in this study were performed using 1.5 T MRI scanner (Philips Achieva).

- The study comprised 44 (61.11%) males and 28 (38.88%) females The age of the patients ranged from 2 months to 85 years. Infarcts, infective conditions, extra axial mass lesions, intra axial mass lesions, hypoxic ischemic encephalopathy and other conditions like hypertensive encephalopathy, demyelination, metabolic disorders were included in this study.
- Infarcts comprised the majority of lesions at 32 cases (44.44 of the total cases studied). Of these acute infarcts constituted 19 cases (59.3%); 10 (31.25%) were chronic infarcts and 3 (9.3%) were subacute infarcts. All cases of acute infarcts and 50% of subacute infarcts showed diffusion restriction. None of the chronic infarcts showed true restriction of diffusion. No signal abnormality was noted in 13% of acute infarcts on T2W images. Thus DWI not only helped detect all cases of acute infarcts but also proved to be a useful tool in categorizing the infarcts as acute, chronic and subacute infarcts.
- Among intra axial tumors true restriction was noted in 5 (35.71%) cases. 50% of glioblastoma multiforme showed true diffusion restriction. None of the low grade gliomas or anaplastic astrocytomas showed diffusion restriction. Thus DWI may help in grading gliomas. DWI also provides information of the cellularity of

tumors. 2 (100%) of medulloblastomas and 1(100%) of lymphomas showed diffusion restriction. These tumors are known to have high cellularity.

- The only case of intracerebral abscesses showed true diffusion restriction. This feature of abscesses on DWI has been shown to help differentiate them from cystic or necrotic brain tumors. The cystic or necrotic component of none of the brain tumors included in this study showed diffusion restriction.
- All cases of arachnoid cysts seen in this study had low signal on DWI. This helps differentiate them from epidermoid cysts which were seen to have higher signal on DWI. 4 (80%) of meningiomas showed restricted diffusion in this study likely reflecting their high cellularity.
- All cases of HII showed diffusion restriction. 1 (33%) of these cases showed no signal change on T2WI. Also the extent of abnormality was noted to be more on DWI than on T2WI. Thus DWI is a more sensitive imaging technique than T2WI in the evaluation of HII.
- The only case of extradural empyemas seen in this study showed restricted diffusion.
- Demyelination did not show restricted diffusion reflecting absence of cytotoxic edema in these conditions.

SUMMARY

Thus DWI is a highly sensitive technique in the detection of acute infarcts and in characterizing infarcts as acute, subacute and chronic. DWI is a sensitive modality for detecting HII and shows the extent of involvement better than T2WI. Presence of diffusion restriction is a useful method of differentiating abscesses from necrotic or cystic neoplasms. Restricted diffusion may be a feature of high grade gliomas and may help in their grading. Highly cellular tumors such as lymphomas, medulloblastomas and meningiomas may show restricted diffusion. Arachnoid cysts can be differentiated from epidermoid cysts by the presence of low signal on DWI. PRES and demyelination do no show restricted diffusion probably due to lack of cytotoxic edema.

BIBLIOGRAPHY

1. Haaga JR, Dogra VS, Forsting M, Gilkeson RC, Ha HK, Sundaram M. CT and MRI of whole body. 5th ed. China: Elsevier; 2009. p. 54, 220.
2. Atlas SW, editors. Magnetic resonance imaging of the brain and spine. 4th ed. China: Lippincott Williams and Wilkins; 2009. p. 472-474.
3. Tadeusz WS, Philipe D, Robert RL, Christo C, Katrijn LV, Alex M et al. Differential diagnosis of bright lesions on diffusion weighted MR images. Radiographics 2003; 23.
4. Tadeusz WS, Cristo C, Alex M, Wael MS, Katrijn VR, Robert L et al. Diffusion weighted MR images of intracerebral masses – comparison with conventional MR. AJNR 2001; 22: 969-976.
5. Mascalchi M, Filippi M, Floris R, Fonda C, Gasparotti R, Villari N. Diffusion MR imaging: clinical applications. Radiol Med 2005 march; 109 (3): 155-197.
6. Chang SC, Lai PH, Chen WL, Weng HH, Ho JT, Wang JS et al. Diffusion weighted MRI features of brain abscess and cystic or necrotic tumors – comparison with conventional MRI. Clinical imaging 2002 July; 26(4): 227-236.
7. Karaarslan E, Arslan A. diffusion weighted MRI in non infarct lesions of the brain. European journal of radiology 2008; 65:402-416.
8. Moritani T, Shrier DA, Numaguchi Y. diffusion-weighted echoplanar MR imaging: clinical application and pitfalls – a pictorial essay. Clinical imaging 2000; 24; 181-92.
9. Tievsky AL, Ptak T, Farkas J. investigation of apparent diffusion coefficient and diffusion tensor anisotropy in acute and chronic multiple sclerosis lesions. AJNR 1999;20(8):1491-9.

10. Cruz Ch, Gasparetto El, Domingues RC. Diffusion weighted MRI in brain tumor. Neuroimaging clinics 2011 February; 21(1):27-49.
11. Wolf RL, Zimmerman RA, Clancy R, Haselgrove JH. Quantitative apparent diffusion coefficient measurement in term neonates for hypoxic ischaemic brain injury: initial response, Radiology 2001 ;218:825-833.
12. Eisenberg RL. Radiology, an illustrated history. St Louis; Mosby; 1992. P. 111-112.
13. Alen PS. Some fundamental principles of nuclear magnetic resonance in medical physics, Monography No. 21: the Physics of MRI. New York: AIP press; 1992. P.15-21.
14. Vlaardingerbroek Mt, Den Boe JA. Magnetic resonance imaging; theory and practice. 3rd ed. New York: Springer; 2002. p. 9-13.
15. Stark DD, William G, Bradley J. Magnetic Resonance Imaging. 3rd ed. Birmingham; Mosby; 2008. P .22-45.
16. Robert B, Lufkin R. the MRI Manual. 2nd ed. New York: Hagendorn ; 2005.p 14-27.
17. LeBihan D. Molecular diffusion nuclear, magnetic resonance imaging. Magnetic Resonance 1991;7(1):30-39.
18. Stejskal Eo, Tanner JE. Spin diffusion measurements; Spin echoes in the presence of time dependent field gradients. Chem Phys 1965; 42:288-292.
19. Susumu Mori, Barker PB. Diffusion magnetic resonance imaging: its principle and applications. The Anatomical Record 1999; 257; 102-109.
20. Hagmann P, Jonasson L, Maeder P, Thiran JP, Weeden VJ, Meuli R. understanding diffusion MR techniques: from scalar diffusion weighted

imaging to diffusion tensor imaging and beyond. Radiogrpahics 2006; 26: 205-223.

21. Abragam A. the principles of nuclear magnetism. London: Oxford University Press; 1961.
22. Bushberg JT, Seibert JA, Edwin M, Leidholdt J, Boone JM. The Essential Physics of Medical Imaging. Baltimore: William and Wilkins; 1994.
23. Rowley HA, Grant PE, Roberts TP. Diffusion MR imaging. Theory and applications. Neuroimaging Clin N Am 1999; 9:343-61.
24. Le Bihan D. Molecular diffusion, tissue micro-dynamics and microstructure. NMR Biomed 1995; 9:375-386.
25. Liu G, Gelderen P, Duyn J, Moonen CT. single-shot diffusion MRI of human brain on a conventional clinical instrument. Magn Reson Med 1996; 35: 671-677.
26. Beaulieu CF, Zhou X, Cofer GP, Johnson GA. Diffusion-weighted MR microscopy with fast spin-echo. Magn Reson Med 1993; 30: 201-206.
27. Gudbjartsson H, Maier SE, Mulkern RV, Morocz IA, Patz S, Jolesz FA. Line scan diffusion imaging. Magn Reson Med 1996; 36: 509-519.
28. Nomura Y, Sakuma H, Takeda k, Tagami t, Okuda Y, Nakagawa T. Diffusional anisotropy of the human brain assessed with diffusion-weighted MR: relation with normal brain development and aging. Am J Neuroradiol 1994; 15:231-238.
29. Wimberger Dm, Roberts TP, Barkovich AJ, Prayer LM, Moseley ME, Kucharczyk J. Identification of “premyelination” by diffusion-weighted MRI. Comput Assist Tomogr 1995; 19:28-33.

30. Le Bihan D. Diffusion and perfusion magnetic resonance imaging: applications to functional MRI. New York: Raven; 1995.
31. Conturo TE, McKinstry RC, Aronovitz JA, Neil JJ. Diffusion MRI: precision, accuracy and flow effects. NMR Biomed 1995; 8:307-332.
32. Gudbjartsson H, Maier SE, Mulkern RV, Morocz IA, Patz S, Jolesz FA. Line scan diffusion imaging. Magn Reson Med 1996; 36: 509-519.
33. Beaulieu CF, Zhou X, Cofer GP, Johnson GA. Diffusion-weighted MR microscopy with fast spin-echo. Magn Reson Med 1993; 30: 201-206.
34. Liu G, Van Gelderen P, Duyn J, Moonen CT. single-shot diffusion MRI of human brain on a conventional clinical instrument. Magn Reson Med 1993; 35: 671-677.
35. Yoshiura T, Wu O, Sorensen AG. Advanced MR techniques: diffusion MR imaging, perfusion MR imaging and spectroscopy. Neuroimaging Clin n Am 1999;9”439-453.
36. Englter ST, Provenzale JM, Parella JR, DeLon DM, Mac Fall JR. The effect of aging on the apparent diffusion coefficient of normal- appearing white matter. Am J Roentgenol 2000; 175:425-430.
37. Terry C, Christopher GF, Robert DZ, Aziz MU. Diffusion changes in the aging human brain. Am J Neuroradiol 2000; 1:1078-1083.
38. Engelbrechi V, Scherer A, Rassek M, Witsack HJ, Modder U. diffusion-weighted MR imaging in the brain in children: findings in the normal brain and in the brain with white matter diseases. Radiology 2002; 222:410-418.
39. Forbes KP, Pipe JG, Bird CR. Changes in brain water diffusion during the 1st year of life. Radiology 202; 222: 405-409.

40. Schafer PW, Grant PE, Gonzalez RG. Diffusion weighted MR imaging of the brain. Radiology 2000 November; 271:331-345.
41. Chien D, Kwong KK, Gress DR, Buonanno FS, Buxton RB, Rosen BR. MR diffusion imaging of cerebral infarction in humans. AM J Neuroradiol 1992; 13:1097-1102.
42. Mintorovitch J, Yang GY, Shimizu H, Kucharczyk J, Chan PH, Weinstein PR. Diffusion-weighted magnetic resonance imaging of acute focal cerebral ischemia; comparison of signal intensity with changes in brain water and Na+, K+ and ATP'ase activity. J Cereb blood Flow Metal 1994; 14:332-336.
43. Schiuer G, Tigges A, Reimer P, Daldrup H, Peters P. The repeatability of MR perfusion studies: a clinical study. International Society for Magnetic Resonance in Medicine, 1995; 84.
44. Le Bihan D, Delennoy J, Levin RL. Temperature mapping with MR imaging of molecular diffusion; application to hyperthermia. Radiology 1989; 171:853-857.
45. Helpen J, Ordidige R, Knight R. The effect of cell membrane water permeability on the apparent diffusion coefficient of water. Society of Magnetic Resonance in Medicine, 1992; 12.
46. Lutsep H, Albers G, DeCrespigny A, Kumar G, Marks M, Moseley M. Clinical utility of diffusion-weighted magnetic resonance imaging in the assessment of ischemic stroke, Neurology 1997;41:574-580.
47. Schwamm L, Koroshetz W, Sorensen A, et al. time course of lesion development in patients with acute stroke: serial diffusion and hemodynamic weighted magnetic resonance imaging. Stroke 1998; 29:2268-2276.

48. Marks M, Tong DC, Beaulieu C, Abers GW, De Crespigny A, Moseley ME. Evaluation of early reperfusion and i.v tPA therapy using diffusion and perfusion weighted MRI. Neurology 1999; 52: 1792_1798.
49. Nagesh V, Welch KM, Windham JP, et al. Time course of ADC changes in ischemic stroke: beyond the human eye. Stroke 1998; 26: 807-812.
50. Mohr J, Biller J, Hilal S, et al. Magnetic resonance versus computed tomographic imaging in the acute stroke. Stroke 1995; 26: 807-812.
51. Bryan R, Levy l, Whitlow W, Killian J, Perziosi T, rosario J. Diagnosis of acute cerebral infarction: comparison of CT and MR imaging. AJNR AM J Neuroradiol 1991; 12:611-620.
52. Gonzalez RG, Schaefer PW, Buonanno FS, et al. Diffusion-weighted MR imaging: diagnostic accuracy in patients imaged within 6 hours of stroke symptom onset. Radiology 1999; 210:155-162.
53. Lovblad K, Laubach H, Baird A, et al. Clinical experience with diffusion-weighted MR in patients with acute stroke. AJNR Am J Neuroradiol 1998; 19: 1061-1066.
54. Singer M, Chong J, Lu D, Schonewille W, Tuhrim S, Atlas S. Diffusion-weighted MRI in acute subcortical infarction. Stroke 1998; 29: 133-136.
55. Barber P, Darby D, Desmond P, et al. Prediction of stroke outcome with echoplanar perfusion and diffusion-weighted MRI. Neurology 1998; 51: 418-456.
56. Lovblad K, Baird A, Schlaug G, et al. Ischemic lesion volumes in acute stroke by diffusion-weighted magnetic resonance imaging correlation with clinical outcome. Ann Neurol 1997; 42: 164-170.

57. Everdingen KJ, Grond J, Kapelle LJ, Ramos LM, Mali WP. Diffusion-weighted magnetic resonance imaging in acute stroke. Stroke 1998; 29: 1783-1790.

58. Ay H, Buonanno F, Schaefer P, et al. Clinical and diffusion-weighted imaging characteristics of an identifiable subset of TIA patients with acute infarction. American Heart Association 1999; 74.

59. Kidwell Cs, Alger JR, DiSalle F, et al. Diffusion MRI in patients with transient ischemic attacks. Stroke 1999; 162:671-677.

60. Tien R, Felsberg G, Friedman H, Brown M, MacFall J. MR imaging of high grade gliomas: value of diffusion-weighted echo-planar pulse sequences. Am J Roentgenol 1994; 162:671-677.

61. Schwartz R, Mulkern r, Gudbjartsson H, Jolesz F. Diffusion-weighted MR imaging in hypertensive encephalopathy: clues to pathogenesis. Am J Neuroradiol 1998; 19: 859-862.

62. Osborn AG, Salzman KL, Barkovich AJ, Katzman GL, Provenzale JM, Hansberger HR et al. Diagnostic imaging brain. 2nd ed Canada Amirsys; 2010.

63. Fu JH, Xue XD, Mao J, Chen LY, Wang XM. Early assessment of severe hypoxic-ischemic encephalopathy in neonates by diffusion-weighted magnetic resonance imaging techniques and its significance. Zonghua er ke za zhi 2007 Nov;45(11):843-847.

64. Tsurdu J, Chew W, Moseley m, Norman d. Diffusion-weighted MR imaging of the brain: value of differentiating between extra-axial cysts and epidermoid tumors.

65. Maeda M, Kawamura Y, Tamagawa Y et al. Intravoxel incoherent motion (IVIM) MRI in intracranial, extra-axial and cysts. J Comput Assist Tomogr 1992; 16:614-518.
66. Els T, Eis M, Hoehn-Berlage M, hossmann K. Diffusion-weighted imaging of experimental brain tumors in rats. MAGMA 1995; 3:13-20.
67. Schefer P, Wang B, Gonzalez R. Echo planar diffusion weighted imaging in pyogenic infections. American Society of Neuroradiology 1997; 103.
68. Kim Y, Chang K, Kim H, Seong S, Kim Y, Han M. Brain abscess and necrotic or cystic brain tumor: discrimination with signal intensity on diffusion-weighted MR imaging. AM J Roentgenol 1998; 171:1487-1490.
69. Yilmaz K, Nevzat K, Alpay A. the role of diffusion weighted echo planar MRI in central nervous system infections regarding etipathogeneses. Diagnostic and interventional journal 2010; 69: 64-33.
70. Brunberg J, Chenevert T, McKeever P et al. In vivo MR determination of water diffusion coefficients and diffusion aniotropy: correlation with structural alteration in gliomas of the cerebral hemispheres. Am J Neuroradiol 1995; 16:361-371.
71. Bahn M, Kido D, Lin W, Pearlman A. Brain magnetic resonance diffusion abnormalities in Creutzfeldt-Jakob disease. Arch Neurol 1997; 54:1411-1415.
72. Schaefer P, Grant E, Wang b, Gonzalez R. Echo planar diffusion weighted imaging in Creutzfeldt-Jakob disease. American Society of Neuroradiology, 1999; 161.
73. Brown p, Cathala F, Castaigne P, Gajdusek DC. Creutzfeldt-Jakob disease: clinical analysis of a consecutive series of 230 neuropathologically verified cases. Annn Neurol 1986; 20: 597-602.

74. Johnson R, Gibbs C. Creutzfeldt-Jakob disease and related transmissible spongiform encephalopathies. N Eng J Med 1998; 339: 1994-2004.

75. Finenstaedt M, Szudra A, Zerr I, et al. MR imaging of Creutzfeldt-Jakob disease. Radiology 1996; 199:793-798.

76. Christiansen P, Gideon P, Thomsen C, stubgaard m, Henricksen O, Larsson H. Increased water self-diffusion in chronic plaques and in apparently normal white matter in patients with multiple sclerosis. Acta Neurol Scand 1993; 87:195-199.

77. Larsson h, Thomsen C, Fredriksen J, Stubgaard M, Henriksen O. In vivo magnetic resonance diffusion measurement in brain of patients with multiple sclerosis. Magn Reson Imaging 1992;10:7-12.

78. Horsfield M, Lai m, Webb S, et al. Apparent diffusion coefficients in benign and secondary progressive multiple sclerosis by nuclear magnetic resonance. Magn Reson Med 1996; 36: 393-400.

79. Allen IV, McKeown SR. A histological, histochemical and biochemical study of the macroscopically normal white matter in multiple sclerosis. J Neurol Sci 1979; 41:81-91.

80. K Rima,G Rohit, P Anjali, C Veena. Role of diffusion weighted MR imaging in early diagnosis of cerebral infarction. Ind J Radiol Imag 2003; 3(2):213-217.

81. Van der Zwam A, Hillen B, Tulleken H et al. Variability of the major cerebral arteries. J Neurosurg 1992; 77: 927-940.

82. Mortani t, Ekholm S, Westesson PL. Diffusion weighted MR imaging of the brain. 2nd ed. London: Springer Science Business Media; 2009. P. 18-84.

83. Catherine Westbrook, .*Handbook of MRI Technique*.4th Edition. John Wiley & Sons, Ltd: 2014. p 48, 63, 64, 72.

84. K.J. van Everdingen,J. van der Grond,L.J. Kappelle, L.M.P. Ramos, W.P.T.M. Mali. Diffusion-Weighted Magnetic Resonance Imaging in Acute Stroke. Stroke.1998; 29: 1783-1790.

85. Augustin M, Bammer R, Simbrunner J, Stollberger R, Hartung HP, Fazekas F Diffusion-weighted imaging of patients with subacute cerebral ischemia: comparison with conventional and contrast-enhanced MR imaging: Am J Neuroradiol. 2000 Oct;21(9):1596-602.

86. Alexander M. McKinneya, Mehmet Teksama, Ross Felicea, Sean O. Caseya,Ronald Cranforda, et al. Diffusion-Weighted Imaging in the Setting of Diffuse Cortical Laminar Necrosis and Hypoxic-Ischemic Encephalopathy. Am J Neuroradiol.: 2004 25: 1659-1665.

87. Choi HY, Choi DS, Ryoo JW, Cho JM, Ko ES, Shin TB, et al.Diffusion-weighted MR Imaging of Hypoxic-Ischemic Encephalopathy.J Korean Soc Magn Reson Med. 2008 Jun;12(1):49-54.

ANNEXURES-I

ETHICAL CLEARANCE

Institutional Ethical Committee
BIJAPUR-586 103.
OUTWARD
No. 50/13
Date. 14-11-13
BLDE (U's Shri B.M. Patil Medical College)

B.L.D.E. UNIVERSITY'S
SHRI.B.M.PATIL MEDICAL COLLEGE, BIJAPUR-586 103
INSTITUTIONAL ETHICAL COMMITTEE

INSTITUTIONAL ETHICAL CLEARANCE CERTIFICATE

The Ethical Committee of this college met on 13-11-2013 *at* 3-30pm *to scrutinize the Synopsis of Postgraduate Students of this college from Ethical Clearance point of view. After scrutiny the following original/corrected & revised version synopsis of the Thesis has been accorded Ethical Clearance.*

Title "Diffusion weighted magnetic resona-nce imaging features of intracranial lesions" ——x——x——

Name of P.G. student Dr Puneet Shirbur.
Department of Radiodiagnosis

Name of Guide/Co-investigator Dr R.C. Pattanashetti
Prof & HOD of Radiodiagnosis

DR.TEJASWINI. VALLABHA
CHAIRMAN
INSTITUTIONAL ETHICAL COMMITTEE
BLDEU'S, SHRI.B.M.PATIL
MEDICAL COLLEGE, BIJAPUR.

Following documents were placed before E.C. for Scrutinization
1) Copy of Synopsis/Research project.
2) Copy of informed consent form
3) Any other relevant documents.

ANNEXURES II

PROFORMA

Name

Age

Sex

Imaging Findings

Extra axial v/s Intra axial

DWI signal intensity

ADC signal intensity

T2 FLAIR signal intensity

ANNEXURE – III

SAMPLE INFORMED CONSENT FORM

B.L.D.E.U.'s SHRI B.M. PATIL MEDICAL COLLEGE HOSPITAL AND RESEARCH CENTRE, VIJAYAPUR – 586103, KARNATAKA

TITLE OF THE PROJECT:	DIFFUSION WEIGHTED MAGNETIC RESONANCE IMAGING FEATURES OF INTRACRANIAL LESIONS
PRINCIPAL INVESTEGATOR:	DR. PUNEET SHIRBUR DEPARTMENT OF RADIO DIAGNOSIS *Email: dr.psshirbur@gmail.com*
PG GUIDE:	DR. R.C PATTANSHETTI PROFESSOR DEPARTMENT OF RADIO-DIAGNOSIS SHRI B.M. PATIL Medical College & Research Centre, Sholapur Road, VIJAYAPUR - 586103

PURPOSE OF RESEARCH:

I have been informed that this study will be to study the **diffusion weighted magnetic resonance imaging features of intracranial lesions.**

I have been explained about the reason for doing this study and selecting me/my ward as a subject for this study. I have also been given free choice for either being included or not in the study.

PROCEDURE:

I/my ward have been explained that, I/my ward will be subjected to 1.5T MRI of brain.

RISKS AND DISCOMFORTS:

I/my ward understand that I/my ward may experience some claustrophobic sensation during the procedure. I/my ward understand that necessary measures will be taken to reduce these complications as and when they arise.

BENEFITS:

I/my ward understand that my participation in this study will help to study diffusion weighted magnetic resonance imaging features of intracranial lesions

CONFIDENTIALITY:

I/my ward understand that medical information produced by this study will become a part of this Hospital records and will be subjected to the confidentiality and privacy regulation of this hospital. Information of a sensitive, personal nature will not be a part of the medical records, but will be stored in the investigator's research file and identified only by a code number. The code key connecting name to numbers will be kept in a separate secure location.

If the data are used for publication in the medical literature or for teaching purpose, no names will be used and other identifiers such as photographs and audio or video tapes will be used only with my special written permission. I understand that I may see the photograph and videotapes and hear audiotapes before giving this permission.

REQUEST FOR MORE INFORMATION:

I understand that I may ask more questions about the study at any time. Dr. Puneet Shirbur is available to answer my questions or concerns. I/my ward understand that I will be informed of any significant new findings discovered during the course of this study, which might influence my continued participation.

If during this study, or later, I wish to discuss my participation in or concerns regarding this study with a person not directly involved, I am aware that the social worker of the hospital is available to talk with me and that a copy of this consent form will be given to me for careful reading.

REFUSAL OR WITHDRAWAL OF PARTICIPATION:

I/my ward understand that my participation is voluntary and I may refuse to participate or may withdraw consent and discontinue participation in the study at any time without prejudice to my present or future care at this hospital.

I/my ward also understand that Dr. Puneet Shirbur will terminate my participation in this study at any time after he has explained the reasons for doing so and has helped arrange for my continued care by my own physician or therapist, if this is appropriate.

INJURY STATEMENT:

I understand that in the unlikely event of injury to me/my ward, resulting directly to my participation in this study, if such injury were reported promptly, then medical treatment would be available to me, but no further compensation will be provided.

I understand that by my agreement to participate in this study, I am not waiving any of my legal rights.

I have explained to _____ the purpose of this research, the procedures required and the possible risks and benefits, to the best of my ability in patient's own language.

Date: Dr. R.C Pattanshetti Dr. Puneet Shirbur

(Guide) (Investigator)

MASTER CHART

Sl. No	Age	Sex	Diagnosis	DWI	ADC	T2 FLAIR	Extra/ Intra-axial
1.	65Y	M	Arachnoid cyst	Hypo	Hyper	Hypo	extra-axial
2.	4Y	F	NCC	Iso	Hyper	Hyper	intra-axial
3.	4Y	F	Tuberculoma	Hyper	Hypo	Hyper	intra-axial
4.	50Y	M	Schwanomma	Iso	Hyper	Hyper	intra-axial
5.	66Y	M	Acute Infarct	Hyper	Hypo	Hyper	intra-axial
6.	63Y	M	Abscess	Hyper	Hypo	Hyper	intra-axial
7.	63Y	M	Subacute infarct	Hyper	Hyper	Hyper	intra-axial
8.	3M	M	HII	Hyper	Hypo	Hyper	intra-axial
9.	44Y	M	NCC	Iso	Hyper	Hyper	intra-axial
10.	44Y	M	Tuberculoma	Hyper	Hyper	Hyper	intra-axial
11.	57Y	F	Acute infarct	Hyper	Hypo	Iso	intra-axial
12.	65Y	F	Chronic infarct	Hypo	Hyper	Hypo	intra-axial
13.	54Y	F	Low grade Glioma	Iso	Hyper	Hyper	intra-axial

14.	70Y	M	Subacute infarct	Hyper	Hyper	Hyper	intra-axial
15.	58Y	M	Tuberculoma	Hyper	Hypo	Hyper	intra-axial
16.	58Y	M	Low grade Glioma	Iso	Hyper	Hyper	intra-axial
17.	59Y	M	Acute infarct	Hyper	Hypo	Hyper	intra-axial
18.	35Y	M	Medulloblastoma	Hyper	Hypo	Hyper	intra-axial
19.	80Y	F	Meningioma	Hyper	hypo	Iso	extra-axial
20.	2M	M	HII	Hyper	Hypo	Iso	intra-axial
21.	65Y	M	Tuberculoma	Hyper	Hypo	Hyper	intra-axial
22.	80Y	F	Acute infarct	Hyper	Hypo	Hyper	intra-axial
23.	70Y	M	Acute infarct	Hyper	Hypo	Hyper	intra-axial
24.	60Y	M	Acute infarct	Hyper	Hypo	Hyper	intra-axial
25.	3Y	M	HSV encephalitis	Hyper	Hyper	Hyper	intra-axial
26.	30Y	M	Extradural empyema	Hyper	Hypo	Hyper	extra-axial
27.	35Y	M	Subacute Infarct	Hyper	Hypo	Hyper	intra-axial

28.	68Y	F	Low grade glioma	Hyper	Hyper	Hyper	intra-axial
29.	65Y	F	Meningioma	Hyper	Hypo	Hyper	extra-axial
30.	60Y	F	Acute infarct	Hyper	Hypo	Iso	intra-axial
31.	3Y	F	HII	Hyper	Hypo	Hyper	intra-axial
32.	60Y	F	Acute infarct	Hyper	Hypo	Hyper	intra-axial
33.	68Y	M	Acute infarct	Hyper	Hypo	Hyper	intra-axial
34.	11Y	M	Medulloblastomas	Hyper	Hypo	Hyper	intra-axial
35.	76Y	M	Acute infarct	Hyper	Hypo	Hyper	intra-axial
36.	45Y	F	Epidermoid	Hyper	Hypo	Hypo	extra-axial
37.	62Y	M	Chronic infarct	Hypo	Hyper	Hypo	intra-axial
38.	80Y	F	Acute infarct	Hyper	Hypo	Hyper	intra-axial
39.	50Y	M	Arachnoid cyst	Hypo	Hyper	Hypo	extra-axial
40.	65Y	M	Acute infarct	Hyper	Hypo	Hyper	intra-axial
41.	5Y	M	Arachnoid cyst	Hypo	Hyper	Hypo	extra-axial

42.	50Y	M	Glioblastoma multiforme	Hyper	Hypo	Hyper	extra-axial
43.	65Y	F	Acute infarct	Hyper	Hypo	Iso	intra-axial
44.	72Y	F	Periventricular leukomalacia	Iso	Hyper	Hyper	intra-axial
45.	45Y	M	Meningioma	Hyper	Hyper	Hyper	extra-axial
46.	35Y	M	Multiple Sclerosis	Iso	hyper	Hyper	intra-axial
47.	6Y	M	Pilocytic astrocytoma	Iso	Hyper	Hypo	intra-axial
48.	65Y	M	Anaplastic astrocytoma	Hyper	Hyper	Hyper	intra-axial
49.	56Y	F	Chronic infarct	Hypo	Hyper	Hypo	intra-axial
50.	70Y	F	ADEM	Iso	Iso	Hyper	intra-axial
51.	60Y	F	Lymphoma	Hyper	Hypo	Hyper	intra-axial
52.	21Y	M	PRES	Iso	Hyper	Hyper	intra-axial
53.	60Y	F	Chronic infarct	Hypo	Hyper	Hypo	intra-axial
54.	61Y	F	Glioblastoma multiforme	Hyper	Hypo	Hyper	intra-axial
55.	57Y	F	Chronic infarct	Hypo	Hyper	Hypo	intra-axial

56.	65Y	F	Acute infarct	Hyper	Hypo	Hyper	intra-axial
57.	60Y	M	Acute infarct	Hyper	Hypo	Hyper	intra-axial
58.	60Y	M	Chronic infarct	Hyper	Hyper	Hyper	intra-axial
59.	50Y	M	Meningioma	Hyper	Hypo	Hyper	extra-axial
60.	45Y	F	Hemangioblastoma	Iso	Hyper	Hyper	intra-axial
61.	65Y	M	Glioblastoma multiforme	Hyper	Hyper	Hyper	intra-axial
62.	53Y	M	Acute infarct	Hyper	Hypo	Hyper	intra-axial
63.	36Y	M	Chronic infarct	Hyper	Hyper	Hyper	intra-axial
64.	17Y	F	Chronic infarct	Hyper	Hyper	Hyper	intra-axial
65.	85Y	F	Chronic infarct	Hyper	Hyper	Hyper	intra-axial
66.	82Y	M	Acute Infarct	Hyper	Hypo	Hyper	intra-axial
67.	60Y	F	Acute infarct	Hyper	Hypo	Hyper	intra-axial
68.	58Y	M	Acute infarct	Hyper	Hypo	Hyper	intra-axial
69.	78Y	M	Glioblastoma multiforme	Hyper	hyper		extra-axial

70.	50Y	M	Chronic infarct	Hyper	Hyper	Hyper	intra-axial
71.	55Y	M	Anaplastic astrocytoma	Hyper	Hyper	Hyper	intra-axial
72.	50Y	F	Meningioma	Hyper	Iso	Iso	extra-axial